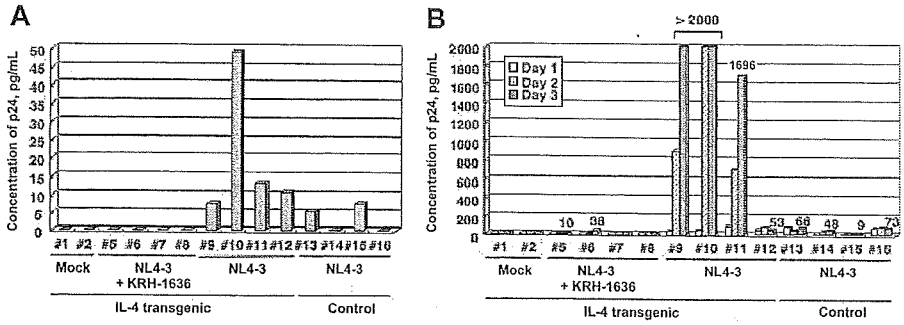

Figure 2. Efficient infection of interleukin (IL)–4–producing hu-PBL-SCID mice with X4 laboratory strain and an inhibitory effect of the CXCR4 antagonist KRH-1636 on infection. Twelve IL-4–transgenic and 4 nontransgenic (control) hu-PBL-SCID mice were generated on the C.B-17-*scid* background. Among them, 8 IL-4–transgenic and 4 control mice were infected intraperitoneally (ip) with the X4 laboratory strain (HIV-1_{NL4-3}) and 4 IL-4–transgenic mice were mock-infected at 1 day after engraftment. To evaluate the effect of KRH-1636, this drug was administered ip twice, at 1 h before and 1 day after infection of 4 IL-4–transgenic mice (NL4-3 + KRH-1636). At 8 days after infection, peritoneal lavage fluids were obtained from the mice in each group. Cells were isolated from the fluids and cultured in IL-2–containing medium. Levels of HIV-1 p24 in the peritoneal lavage fluids *(A)* and culture supernatants at days 1–3 after incubation *(B)* were quantitated for infectivity and replication efficiency by ELISA. With regard to the data on mock-infected mice, only 2 of 4 representative data are presented. The nos. listed above the bars in the graph indicate levels of HIV-1 p24 when it was detectable on day 3 (most of the values were <200 pg/mL, and select samples showed values of >2000 pg/mL). Pound signs (#) indicate mouse nos. Results shown are representative of 3 independent experiments.

IL-4–transgenic C.B-17-*scid* mice are susceptible but also demonstrate that the virus from such cells is replication competent. In addition, these findings suggest that the use of intracellular p24 levels is not a sensitive enough technique and that data using the intracellular p24 assay need to be carefully evaluated. These data also indicate that the IL-4–transgenic hu-PBL-SCID mice provide a powerful model for the study of X4 HIV-1 infection independently of the genetic background of the mice.

Inhibitory effect of the CXCR4 antagonist on infection of IL-4–transgenic hu-PBL-SCID mice with the X4 laboratory strain. In an effort to further validate that the CXCR4 coreceptor was indeed used by the X4 HIV-1 virus in the IL-4–transgenic hu-PBL-SCID mice, we used the X4 virus-entry inhibitor, CXCR4 antagonist KRH-1636. Thus, the IL-4–transgenic hu-PBL-SCID mice on the C.B-17-*scid* background were infected with X4 laboratory strain HIV-1_{NL4-3} and were either mock treated or treated with KRH-1636, and the peritoneal lavage fluids, cells in fluids, and cell-culture supernatants were examined as described above. As shown in table 2, the frequency of $CXCR4^+CD4^+$ cells in KRH-1636–treated IL-4–transgenic mice was marginally lower than that in mock-treated IL-4–transgenic mice. In addition, the MFI of CXCR4 expression by the $CD4^+$ T cells was clearly reduced by KRH-1636 administration. Importantly, treatment with KRH-1636 almost completely blocked X4 HIV-1 infection in these IL-4–transgenic mice (figure 2). These data indicate that X4 HIV-1 infection in transgenic mice is CXCR4 dependent and that our mouse model can be used to develop and test new anti-X4 HIV-1 drugs in vivo.

Therapeutic effect of KRH-1636 on the infection of IL-4–transgenic hu-PBL-SCID mice with MDR clinical isolates. The appearance of MDR HIV-1 clinical isolates has been and continues to be one of the growing problems in a significant number of patients receiving HAART and seriously limits the use of the antiviral drugs that are currently available. Thus, the development of novel adjunct or alternative therapeutics is an urgent need. Since treated patients tend to harbor significantly higher levels of either dual/mixed or X4 viruses [23] and since MDR isolates are not usually refractory to new treatment with drugs from classes that have not been used previously in patients from which the viruses were derived, we finally wanted to examine the effect of KRH-1636 on MDR HIV-1 infection in IL-4–transgenic hu-PBL-SCID mice. For this experiment, we used the IL-4–transgenic BALB/cA-dKO mice instead of the IL-4–transgenic C.B-17-*scid* mice, because the former seems more permissive to X4 HIV-1 infection than the latter, as described above. Before the in vivo study, we confirmed that the in vitro infection by 3 MDR clinical isolates could be inhibited with KRH-1636 (more than ~90% inhibition at the 5-μmol/L level). Thus, groups of IL-4–transgenic hu-PBL-SCID mice were infected with a mixture of these selected MDR isolates containing equal IU of each virus and treated with KRH-1636 or the tartrate carrier control. Thereafter, the cells obtained from the peritoneal lavage fluids were analyzed for the expression of cell-surface human CD4, CD3, and intracellular p24. The serum, peritoneal lavage fluids, and supernatants following in vitro culture of the cells for 24 h were assayed for levels of p24 production. Flow cytometry analysis after CD4 staining demonstrated a significant decline in $CD4^+$ T cells in 2 (mouse 7 and mouse 8) of 4 control-treated mice (figure 3*A;* top profile shows data from 1 of these 2 mice), which was likely due to MDR HIV-1 pathogenesis. However, importantly, no detectable depletion of $CD4^+$ T cells was observed in any of 4 KRH-1636–treated mice (figure 3*A;* bottom profile). As summarized in table 3, the difference in the frequency of $CD4^+$ T cells between the control-treated mice and the

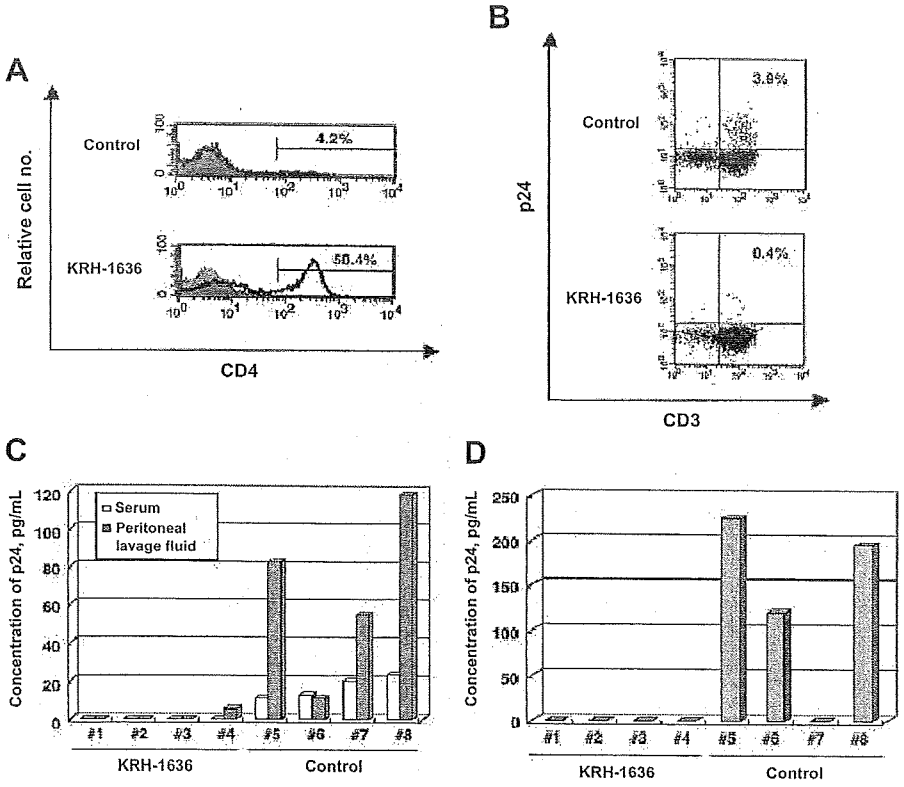

Figure 3. Prophylactic effect of KRH-1636 on infection and pathogenesis by multidrug-resistant (MDR) HIV-1 clinical isolates. Eight interleukin (IL)–4–transgenic hu-PBL-SCID mice (BALB/cA-dKO) were infected intraperitoneally (ip) with a mixture of MDR HIV-1 clinical isolates at 1 day after human peripheral blood mononuclear cell transfer. In an effort to assess the effect of KRH-1636 on HIV-1 infection, this agent or tartrate (control drug) was administered to 4 mice per group ip twice, at 1 h before infection and 1 day after infection. At 7 days after infection, serum and peritoneal lavage fluids were harvested from mice in each group, and cells were collected from the fluids. *A*, Cells examined for human CD4 expression by cell-surface staining and standard flow cytometry. Representative data from a single mouse from the control-treated or the KRH-1636–treated HIV-1–infected mice are shown. The frequency of $CD4^+$ T cells is depicted by a thick line, and the background control is depicted by a thin line with gray shading. The nos. above the bars indicate the percentage of positive cells. *B*, Aliquot of the peritoneal lavage cells analyzed by flow cytometry for the frequency of $CD3^+$ T cells that were positive for the intracellular presence of HIV-1 p24. Representative data of cells from the control-treated and the KRH-1636–treated HIV-1–infected mice are shown. The nos. in the graphs indicate the percentage of $CD3^+p24^+$ cells. *C*, Concentrations of p24 in serum and peritoneal lavage fluid. Concentrations were determined by ELISA to quantify MDR HIV-1 infection and replication efficiency. Pound signs (#) indicate mouse nos. *D*, Levels of in vitro p24 production. The remaining cells were cultured in a microtiter plate containing $IL\text{-}2^+$ medium for ~24 h, and the culture supernatants obtained were assayed for levels of in vitro p24 production by ELISA. Pound signs (#) indicate mouse nos. Results shown are representative of 3 similar independent experiments.

KRH-1636–treated mice was not significant. However, the MFI of CD4 expression was significantly decreased in the control-treated mice (229.3 vs. 296.3; $P < .05$). Results of CD3/p24 staining showed that the frequency of $CD3^+p24^+$ cells was markedly inhibited in the KRH-1636–treated mice, compared with that in the carrier-treated control mice (figure 3*B* and table 3). Furthermore, levels of HIV-1 p24 in the serum samples, peritoneal lavage fluids, and culture supernatants from the KRH-

Table 3. Effect of KRH-1636 on infection and pathogenesis by multidrug-resistant (MDR) HIV-1 clinical isolates in interleukin (IL)–4–transgenic hu-PBL-SCID mice.

BALB/cA-dKO mice	X4 HIV-1 infection	CXCR4 antagonist	Mice, no.	$CD4^+$ T cells, %	*P*	$CD4^+$ T cells, MFI	*P*	$p24^+$ T cells, %	*P*
IL-4 transgenic	MDR	Control	4	14.7 ± 11.9	NS	229.3 ± 33.0	<.05	3.2 ± 0.8	<.01
IL-4 transgenic	MDR	KRH-1636	4	31.3 ± 15.7		296.3 ± 25.2		0.8 ± 0.7	

NOTE. IL-4–transgenic hu-PBL-SCID mice on the BALB/cA-dKO background were infected with MDR HIV-1 clinical isolates and administered tartrate (control) or KRH-1636. Cells in peritoneal lavage fluid from the mice in each group were stained with appropriate monoclonal antibodies and analyzed by flow cytometry, as described in Methods. Data shown here are mean ± SD values. MFI, mean fluorescence intensity; NS, not significant. The indicated *P* values for the comparison between control mice and mice that received KRH-1636 are based on Student's *t* test.

1636–treated HIV-1–infected mice were almost completely reduced relative to those in the control mice (figure 3*C* and 3*D*). Note that the failure to detect the in vitro production of p24 in mouse 7 might result from depletion of $CD4^+$ T cells (figure 3*D*). These data demonstrate that the CXCR4 antagonist KRH-1636 has a marked degree of prophylactic effect on infection with pathogenic MDR clinical isolates in vivo.

DISCUSSION

Humanized mice that have served as valuable small animal models include the SCID-hu Thy/Liv mouse [24–28]. This mouse model, generated by implanting human hematopoietic tissues (human fetal thymus/liver) under the kidney capsule, has been used for the study of HIV-1 and is known for permissiveness to X4 HIV-1 infection [26–28]. However, the use of this model is limited by the fact that the implants are of human fetal organ origins that are not easily available. On the other hand, the hu-PBL-SCID mouse model provides another surrogate in vivo HIV-1 infection assay system. Although this model has led to a number of successful studies of HIV-1 [8–14], there was still a limitation in that it was difficult to demonstrate X4 HIV-1 infection and replication in such mice. Thus, to add extra value to the use of this mouse system for the study of HIV-1, in the present study we developed novel human IL-4–transgenic hu-PBL-SCID mice that enable CXCR4-using HIV-1 strains to efficiently infect and replicate in these mice.

Human IL-4 has low homology with murine IL-4 both at the gene and protein levels, accounting for the lack of cross-reactivity of this cytokine in the 2 species in vitro [29–32]. Results of the experiments reported here indicate that the high efficiency of X4 HIV-1 infection in the IL-4–transgenic hu-PBL-SCID mice was, at least in part, secondary to enhanced expression of viral receptors induced by human IL-4 synthesized endogenously. Interestingly, although there was no apparent increase in the number of cells recovered from the engrafted transgenic mice, there was a significant increase in the number of $CD4^+$ T cells recovered (1.5–3-fold). It is thus possible that the other cell lineages migrate from the peritoneal cavity to other tissues of the mice, resulting in enrichment of the $CD4^+$ T cell lineage. However, further studies of other tissues are needed to clarify this issue. Furthermore, our preliminary experiments indicate that the IL-4–transgenic hu-PBL-SCID mice remain permissive to R5 strain infection (data not shown).

In this report, we created 2 types of novel hu-PBL-SCID mice by transplanting human PBMCs into IL-4–transgenic C.B-17-*scid* and BALB/cA-dKO mice. The data obtained show that hu-PBL-SCID mice using the IL-4–producing BALB/cA-dKO mice appeared more permissive to X4 HIV-1 infection than did those using the IL-4–producing C.B-17-*scid* mice, at least as determined by the presence of intracellular p24. Although the reasons for this difference remain to be determined, it should be noted that, whereas the BALB/cA-dKO mice were derived by double mutation with defects in both the recombinase-activating gene 2 (Rag-2) and the gene encoding the γ_c chain of select cytokine receptors [19, 20], the C.B-17-*scid* mice have only the Rag-2 mutation [18]. Thus, although the Rag-2 mutation prevents the normal maturation of T and B lymphocytes, the γ_c chain mutation abrogates the expression of functional receptors for IL-2 and other cytokines, preventing the expansion of lymphocytes, including NK cells, which play an important role in the innate immune response such as nonspecific rejection of xenogeneic grafts. It is thus possible that the C.B-17-*scid* mice maintain a low but significant residual level of NK cell function, which may play a role in the difference noted above even though they were administered significant levels of anti–IL-2Rβ antibody. Since the BALB/cA-dKO mice are completely deficient in NK cell lineage and function, they are more immunodeficient than the C.B-17-*scid* mice, suggesting that the level and type of immunodeficiency in the BALB/cA-dKO mice may facilitate better engraftment and more efficient viral infection and propagation within these mice. These select defects of the BALB/cA-dKO mice might render the IL-4–transgenic mouse model on this background more valuable and ideal for studies of X4 HIV-1.

Acknowledgments

We thank the National Institutes of Health AIDS Research and Reference Reagent Program and M. Sasaki for supplying interleukin-2 and technical support, respectively. We are also grateful to Prof. Aftab Ansari for his critical reading of the manuscript and for his helpful discussion about and suggestions for the manuscript.

References

1. Feng Y, Broder CC, Kennedy PE, Berger EA. HIV-1 entry cofactor: functional cDNA cloning of a seven-transmembrane, G protein-coupled receptor. Science 1996; 272:872–7.
2. Alkhatib G, Combadiere C, Broder CC, et al. CC CKR5: a RANTES, MIP-1alpha, MIP-1beta receptor as a fusion cofactor for macrophage-tropic HIV-1. Science 1996; 272:1955–8.
3. Berson JF, Long D, Doranz BJ, Rucker J, Jirik FR, Doms RW. A seven-transmembrane domain receptor involved in fusion and entry of T-cell-tropic human immunodeficiency virus type 1 strains. J Virol 1996; 70: 6288–95.
4. Deng H, Liu R, Ellmeier W, et al. Identification of a major co-receptor for primary isolates of HIV-1. Nature 1996; 381:661–6.
5. Doranz BJ, Rucker J, Yi Y, et al. A dual-tropic primary HIV-1 isolate that uses fusin and the beta-chemokine receptors CKR-5, CKR-3, and CKR-2b as fusion cofactors. Cell 1996; 85:1149–58.
6. Berger EA, Doms RW, Fenyo EM, et al. A new classification for HIV-1. Nature 1998; 391:240.
7. Xiao L, Rudolph DL, Owen SM, Spira TJ, Lal RB. Adaptation to promiscuous usage of CC and CXC-chemokine coreceptors in vivo correlates with HIV-1 disease progression. AIDS 1998; 12:F137–43.
8. Mosier DE. Adoptive transfer of human lymphoid cells to severely immunodeficient mice: models for normal human immune function, autoimmunity, lymphomagenesis, and AIDS. Adv Immunol 1991; 50:303–25.
9. Mosier DE, Gulizia RJ, Baird SM, Wilson DB, Spector DH, Spector SA. Human immunodeficiency virus infection of human-PBL-SCID mice. Science 1991; 251:791–4.

10. Torbett BE, Picchio G, Mosier DE. hu-PBL-SCID mice: a model for human immune function, AIDS, and lymphomagenesis. Immunol Rev **1991**; 124:139–64.
11. Mosier DE, Gulizia RJ, MacIsaac PD, Torbett BE, Levy JA. Rapid loss of CD4+ T cells in human-PBL-SCID mice by noncytopathic HIV isolates. Science **1993**; 260:689–92.
12. Rizza P, Santini SM, Logozzi MA, et al. T-cell dysfunctions in hu-PBL-SCID mice infected with human immunodeficiency virus (HIV) shortly after reconstitution: in vivo effects of HIV on highly activated human immune cells. J Virol **1996**; 70:7958–64.
13. Fais S, Lapenta C, Santini SM, et al. Human immunodeficiency virus type 1 strains R5 and X4 induce different pathogenic effects in hu-PBL-SCID mice, depending on the state of activation/differentiation of human target cells at the time of primary infection. J Virol **1999**; 73:6453–9.
14. Yoshida A, Tanaka R, Murakami T, et al. Induction of protective immune responses against R5 human immunodeficiency virus type 1 (HIV-1) infection in hu-PBL-SCID mice by intrasplenic immunization with HIV-1-pulsed dendritic cells: possible involvement of a novel factor of human $CD4^+$ T-cell origin. J Virol **2003**; 77:8719–28.
15. Jourdan P, Abbal C, Noraz N, et al. IL-4 induces functional cell-surface expression of CXCR4 on human T cells. J Immunol **1998**; 160:4153–7.
16. Tanaka Y, Koyanagi Y, Tanaka R, Kumazawa Y, Nishimura T, Yamamoto N. Productive and lytic infection of human CD4+ type 1 helper T cells with macrophage-tropic human immunodeficiency virus type 1. J Virol **1997**; 71:465–70.
17. Suzuki Y, Koyanagi Y, Tanaka Y, et al. Determinant in human immunodeficiency virus type 1 for efficient replication under cytokine-induced $CD4^+$ T-helper 1 (Th1)- and Th2-type conditions. J Virol **1999**; 73:316–24.
18. Bosma GC, Custer RP, Bosma MJ. A severe combined immunodeficiency mutation in the mouse. Nature **1983**; 301:527–30.
19. Traggiai E, Chicha L, Mazzucchelli L, et al. Development of a human adaptive immune system in cord blood cell-transplanted mice. Science **2004**; 304:104–7.
20. Berges BK, Wheat WH, Palmer BE, Connick E, Akkina R. HIV-1 infection and CD4 T cell depletion in the humanized $Rag2^{-/-}\gamma c^{-/-}$ (RAG-hu) mouse model. Retrovirology **2006**; 3:76.
21. Ichiyama K, Yokoyama-Kumakura S, Tanaka Y, et al. A duodenally absorbable CXC chemokine receptor 4 antagonist, KRH-1636, exhibits a potent and selective anti-HIV-1 activity. Proc Natl Acad Sci USA **2003**; 100:4185–90.
22. Tanaka T, Kitamura F, Nagasaka Y, Kuida K, Suwa H, Miyasaka M. Selective long-term elimination of natural killer cells in vivo by an anti-interleukin 2 receptor beta chain monoclonal antibody in mice. J Exp Med **1993**; 178:1103–7.
23. Hunt PW, Harrigan PR, Huang W, et al. Prevalence of CXCR4 tropism among antiretroviral-treated HIV-1–infected patients with detectable viremia. J Infect Dis **2006**; 194:926–30.
24. Goldstein H, Pettoello-Mantovani M, Katopodis NF, Kim A, Yurasov S, Kollmann TR. SCID-hu mice: a model for studying disseminated HIV infection. Semin Immunol **1996**; 8:223–31.
25. McCune JM. Animal models of HIV-1 disease. Science **1997**; 278:2141–2.
26. Aldrovandi GM, Feuer G, Gao L, et al. The SCID-hu mouse as a model for HIV-1 infection. Nature **1993**; 363:732–6.
27. Berkowitz RD, Alexander S, Bare C, et al. CCR5- and CXCR4-utilizing strains of human immunodeficiency virus type 1 exhibit differential tropism and pathogenesis in vivo. J Virol **1998**; 72:10108–17.
28. Bonyhadi ML, Rabin L, Salimi S, et al. HIV induces thymus depletion in vivo. Nature **1993**; 363:728–32.
29. Yokota T, Otsuka T, Mosmann T, et al. Isolation and characterization of a human interleukin cDNA clone, homologous to mouse B-cell stimulatory factor 1, that expresses B-cell- and T-cell-stimulating activities. Proc Natl Acad Sci USA **1986**; 83:5894–8.
30. Bonsch D, Kammer W, Lischke A, Friedrich K. Species-specific agonist/antagonist activities of human interleukin-4 variants suggest distinct ligand binding properties of human and murine common receptor gamma chain. J Biol Chem **1995**; 270:8452–7.
31. Idzerda RL, March CJ, Mosley B, et al. Human interleukin 4 receptor confers biological responsiveness and defines a novel receptor superfamily. J Exp Med **1990**; 171:861–73.
32. Morrison BW, Leder P. A receptor binding domain of mouse interleukin-4 defined by a solid-phase binding assay and in vitro mutagenesis. J Biol Chem **1992**; 267:11957–63.

Available online at www.sciencedirect.com
ScienceDirect
VIROLOGY
ELSEVIER
Virology 370 (2008) 142–150
www.elsevier.com/locate/yviro

Neutralizing antibodies decrease the envelope fluidity of HIV-1

Shinji Harada [a,*], Kazuaki Monde [a], Yuetsu Tanaka [b], Tetsuya Kimura [a], Yosuke Maeda [a], Keisuke Yusa [a]

[a] *Department of Medical Virology, Graduate School of Medical Sciences, Kumamoto University, Kumamoto 860-8556, Japan*
[b] *Department of Immunology, Graduate School and Faculty of Medicine, University of the Ryukyus, Okinawa 903-0215, Japan*

Received 22 June 2007; returned to author for revision 6 August 2007; accepted 17 August 2007
Available online 27 September 2007

Abstract

For successful penetration of HIV-1, the formation of a fusion pore may be required in order to accumulate critical numbers of fusion-activated gp41 with the help of fluidization of the plasma membrane and viral envelope. An increase in temperature to 40 °C after viral adsorption at 25 °C enhanced the infectivity by 1.4-fold. The enhanced infectivity was inhibited by an anti-CXCR4 peptide, T140, and anti-V3 monoclonal antibodies (0.5 and 694/98-D) by post-attachment neutralization, but not by non-neutralizing antibodies (670-30D and 246-D) specific for the C5 of gp120 and cluster I of gp41, respectively. Anti-HLA-II and an anti-HTLV-I gp46 antibody, LAT27, neutralized the molecule-carrying HIV-$1_{C\text{-}2(MT\text{-}2)}$. The anti-V3 antibodies suppressed the fluidity of the HIV-$1_{C\text{-}2}$ envelope, whereas the non-neutralizing antibodies did not. The anti-HLA-II antibody decreased the envelope fluidity of HIV-$1_{C\text{-}2(MT\text{-}2)}$, but not that of HIV-$1_{C\text{-}2}$. Therefore, fluidity suppression by these antibodies represents an important neutralization mechanism, in addition to inhibition of viral attachment.

Keywords: HIV-1; Neutralizing antibody; Membrane/envelope fluidity; Fusion pore

Introduction

Viral neutralization consists of a decrease in the infectious titer of a viral preparation following its exposure to antibodies. The loss of infectivity is brought about by interference of the antibodies bound to the viruses during any step from viral attachment to the cells to release of the viral genome into the host cells. The potent and broad capacity of the available neutralizing antibodies against human immunodeficiency virus type 1 (HIV-1) has been attributed to inhibition of fusion and/or virus attachment to the cell surface (Klasse and Sattentau, 2002; Zwart et al., 1991). Thus, the neutralization effects are currently well explained by antibody coating of the virions (high-occupancy theory of neutralization) (Klasse and Sattentau, 2002). However, the high-occupancy theory cannot solely account for the post-attachment neutralization (PAN) (Armstrong et al., 1996; Edwards and Dimmock, 2001), synergistic (Zwick et al., 2001) and additive (Verrier et al., 2001) effects of neutralizing antibodies, and HIV-1 neutralization by one or a few antibody molecules (Harada, 2002). Therefore, there must be additional mechanisms involved in HIV-1 neutralization.

Recently, we reported that small changes in the fluidity of the plasma membrane and/or viral envelope would be indispensable for modifying HIV-1 infectivity (Harada et al., 2005). We hypothesized that fluidity-mediated accumulation of fusion-activated domains was required to form a wide fusion pore large enough for an enveloped viral core to pass through. In fact, the increased or decreased fluidity changes observed after different treatments with the same fluidity modulator, such as glycyrrhizin (Harada, 2005) or fattiviracin FV-8 (Harada et al., 2007), were parallel with the high or low susceptibility of the treated cells to HIV-1 infection and fusion. These modulators are broad antiviral agents, which are especially effective against enveloped viruses. Furthermore, they were found to reduce the infectivity of virions when the viruses were pretreated (Harada, 2005; Harada et al., 2007). Notably, this latter finding reminded us of the actions of neutralizing antibodies against viral particles.

* Corresponding author. Fax: +81 96 373 5132.
E-mail address: biodef@gpo.kumamoto-u.ac.jp (S. Harada).

0042-6822/$ - see front matter © 2007 Elsevier Inc. All rights reserved.
doi:10.1016/j.virol.2007.08.021

In order to gain further insights into the functions of membrane/envelope fluidity in HIV-1 infection and neutralization, we designed a series of experiments to examine the effects of neutralizing antibodies on the fluidization of the HIV-1 envelope and plasma membrane. We found that these antibodies suppressed the fluidization of the highly ordered lipid bilayer of the viral envelope when they exerted neutralization against the respective virus. These studies provide novel insights into the cell biology of retroviral penetration and demonstrate distinct roles for membrane fluidity at early stages of HIV-1 penetration.

Results

Neutralization and PAN by the anti-V3, anti-C5 and anti-gp41 monoclonal antibodies

Conventional neutralization experiments were conducted by pre-incubating viruses with the antibodies prior to their addition to cell culture. At 1 g/ml, the 0.5 (anti-V3) monoclonal antibody (mAb) neutralized more than 90% of plaque-cloned HIV-1_{C-2} (C-2 viruses) (Masuda et al., 1990) and X4 envelope-pseudotyped viruses with a luciferase reporter gene (NL43-luc viruses) (Harada et al., 2004b). Next, the neutralization activities of human mAbs against gp120 V3 (694/98-D), gp120 C5 (670-30D) and gp41 cluster I (246-D) were examined. All of these mAbs were previously reported to bind to intact clade B (III_B) virions (Nyambi et al., 2000). As shown in Fig. 1A, 1 g/ml 694/98-D neutralized more than 90% of NL43-luc viruses, similar to 0.5 , whereas 670-30D and 246-D mAbs rather enhanced the infectivity by around 1.3-fold at all concentrations examined. Thus, 0.5 and 694/98-D mAbs are neutralizing antibodies, whereas 670-30D and 246-D are non-neutralizing antibodies.

NL43-luc viruses were incubated with GHOST/CXCR4 cells at 25 °C for 1 h. After this viral adsorption, the post-adsorption steps were carried out at either 37 °C or 40 °C in the presence or absence of the anti-CXCR4 peptide T140 or mAbs (Fig. 1B). T140 inhibited 95% of the infection when GHOST/CXCR4 cells were treated with 1 M T140 before infection with NL43-luc pseudoviruses (Harada et al., 2005). Increasing the temperature to 40 °C during the post-adsorption steps augmented the level of infection by 1.4-fold (Fig. 1B). This phenomenon is hereafter referred to as post-attachment enhancement (PAE). The PAEs were repeatedly observed by 1.5- to 2.0-fold (Harada et al., 2004a, 2005). The PAEs from 25 °C to 40 °C were strongly abrogated by 1 M T140 (Fig. 1B), indicating that T140 could restrain the viruses from forming multiple-site binding or accumulating fusion-activated gp41 domains by occupying CXCR4. The PAE of 1.4-fold observed at 40 °C was also significantly inhibited by 1 g/ml 0.5 or 4 g/ml 694/98-D mAbs (Fig. 1B), suggesting that these anti-V3 mAbs could mediate PAN when the viruses were loosely bound to the cells at 25 °C. An increased amount (10 g/ml) of 0.5 mAb showed the same inhibitory effect (about 30%) on the PAE as 1 g/ml, indicating that the PAE inhibition by this antibody could not be solely explained by

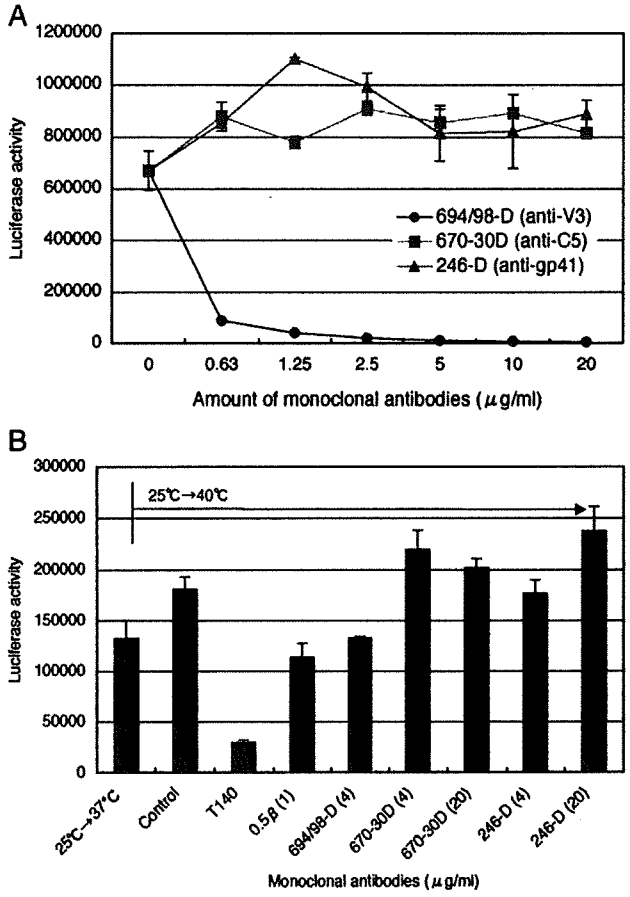

Fig. 1. Conventional neutralization of NL43-luc pseudoviruses by 694/98-D (circles), 670-30D (squares), and 246-D (triangles) mAbs (A), and effects of 1 M T140 and HIV-1-specific mAbs (0.5 , 694/98-D, 670-30D, and 246-D) on PAE at 40 °C for 1 h after viral adsorption at 25 °C (B). All experiments in panels A and B were carried out in triplicate, and solid lines and bars show the mean±SD.

covering the V3 loop of gp120 with antibody molecules, as was the case for T140 occupation of CXCR4. Anti-C5 (670-30D) and anti-gp41 (246-D) mAbs had little effects on the PAN, but tended to enhance the PAE (Fig. 1B).

Suppression of viral envelope fluidization by neutralizing anti-V3 antibodies

The structural and dynamic modification of envelope lipids was examined using a spin-label method (Figs. 2 and 3). As a negative control for C-2, 0.5 -escaped C-2 (esc.C-2) viruses were used. More than 90% of the C-2 viruses were neutralized by 1 g/ml 0.5 , whereas the esc.C-2 viruses were not affected (Masuda et al., 1990). The esc.C-2 viruses have one point mutation in the crown of the V3-loop, resulting in exchange of GPG to GQG. The order parameters of 0.5 -treated C-2 viruses were higher at 25 °C, 37 °C and 40 °C than those of control IgG (MOPC21)-treated viruses (Figs. 2A and B; Fig. 3A), indicating that 1 g/ml 0.5 mAb suppressed the fluidity of the viral envelope. At 37 °C, 0.5 mAb suppressed the fluidity by 7%. However, no such effect of 0.5 was observed in the case of the esc.C-2 viruses (Fig. 3B). Thus, the fluidity suppression by this antibody is consistent

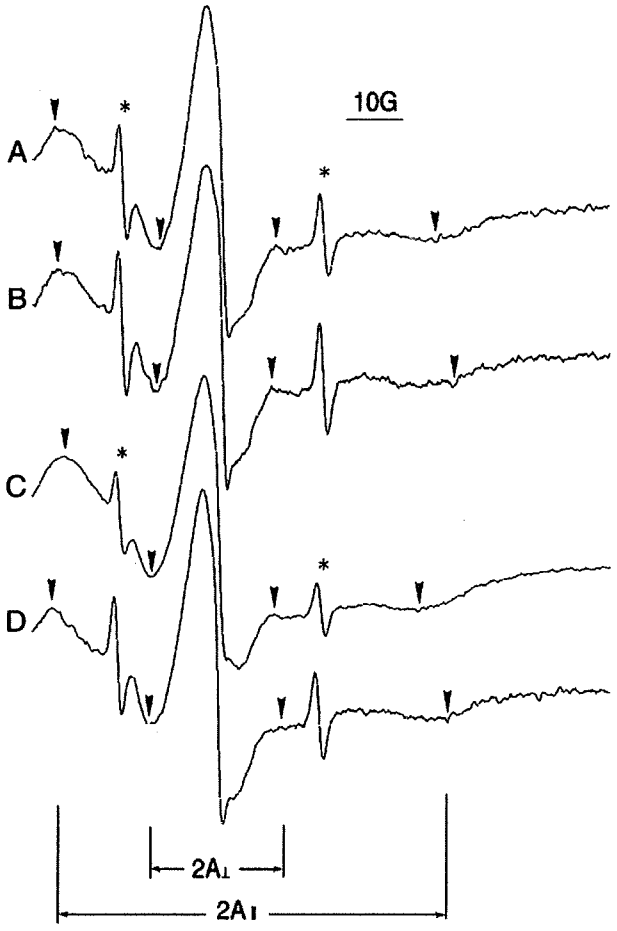

Fig. 2. ESR spectra of viral envelopes from intact C-2 (A), 0.5 -treated C-2 (B), C-2(MT-2) (C), and anti-HLA-II-treated C-2(MT-2) (D) viruses at 37 °C. Viruses (50 ml) were incubated in the presence or absence of 0.5 or anti-HLA-II antibodies at a final concentration of 1 g/ml at 37 °C for 40 min, and then labeled with 5-DSA for 20 min. Virus pellets were examined by ESR spectroscopy. The outer and inner hyperfine splittings, $2A_{//}$ and 2A , were measured as indicated by the arrowheads. Asterisks indicate the spectra of free 5-DSA. The order parameters (S-values) of (A), (B), (C) and (D) are 0.736, 0.787, 0.678, and 0.772, respectively. The scale (10G) of the horizontal axis is shown.

with its neutralization data. Another anti-V3 mAb, 694/98-D (1 g/ml) also suppressed the fluidity of the C-2 envelope (Fig. 3C). However, the non-neutralizing 670-30D (0.5 g/ml) and 246-D (1 g/ml) mAbs had no effects on the fluidization of the viral envelope (Fig. 3C). Similar effects on the plasma membrane fluidity were obtained when MOLT-4/C-2 cells were treated with 0.5 , 694/98-D, 670-30D and 246-D mAbs (data not shown). Thus, the 0.5 and 694/98-D mAbs suppressed the fluidity not only of the viral envelope but also of the plasma membrane.

HIV-1 neutralization by antibodies against non-HIV molecules

Adsorption-blocking, namely, the high-occupancy theory, cannot be completely excluded for the observed inhibition by the 0.5 and 694/98-D mAbs in the neutralization experiments. Therefore, we examined neutralization by non-HIV antibodies.

FACS analyses revealed that MOLT-4 cells did not express HLA-II molecules (Fig. 4A), whereas human T-cell leukemia virus type I (HTLV-I)-transformed MT-2 cells carried many of these molecules on their surface (Fig. 4B). MT-2 cells were also positive for HTLV-I gp46 detected by neutralizing LAT27 and non-neutralizing LAT12 antibodies (Fig. 4C). The binding affinity of LAT27 appeared to be stronger than that of LAT12 (Fig. 4C). HIV-$1_{C\text{-}2(MT\text{-}2)}$ viruses that budded from HIV-$1_{C\text{-}2}$-infected MT-2 cells were expected to have both HLA-II molecules and HTLV-I gp46 as phenotype-mixing progeny viruses. It has been reported that HIV-1 carries more HLA-II molecules than gp120 (Trubey et al., 2003). The anti-HLA-II

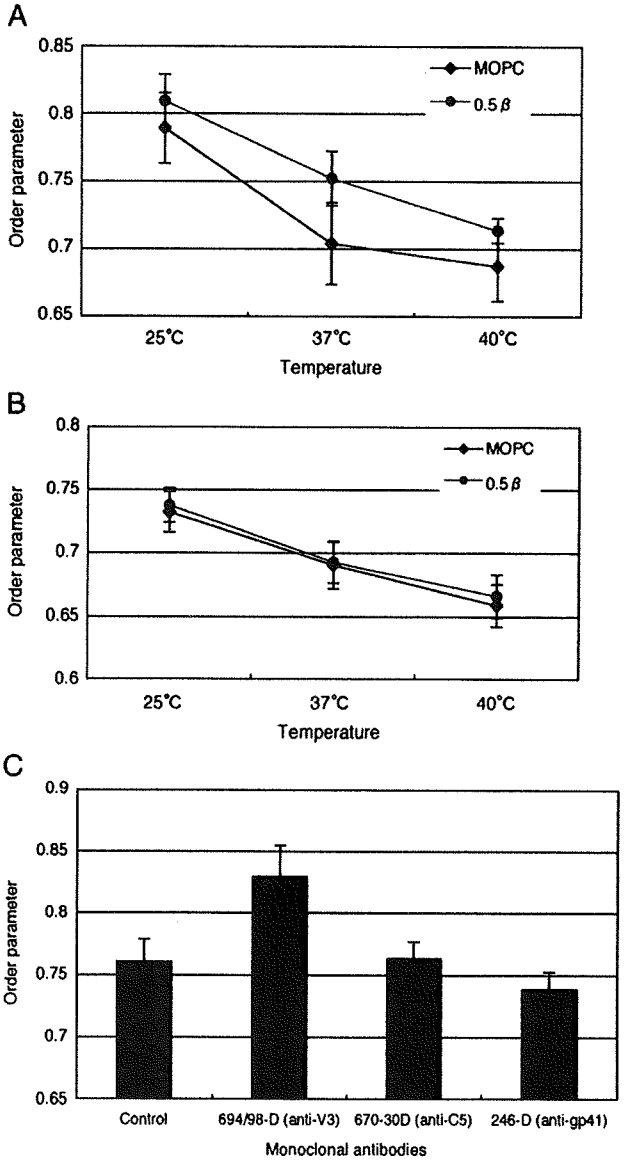

Fig. 3. Effects of 1 g/ml MOPC21 (diamonds) and 1 g/ml 0.5 (circles) on the envelope fluidity of C-2 (A) and esc.C-2 (B) viruses. Viruses (50 ml) were treated with each antibody at 37 °C for 40 min prior to labeling with 5-DSA for 20 min. All measurements were carried out in triplicate and the solid lines show the mean±SD. (C) Effects of 1 g/ml 694/98-D (n=8), 0.5 g/ml 670-30D (n=2), and 1 g/ml 246-D (n=5) on the envelope fluidity of C-2 viruses. As a control, PBS was used instead of an mAb (n=3). Bars show the mean±SD.

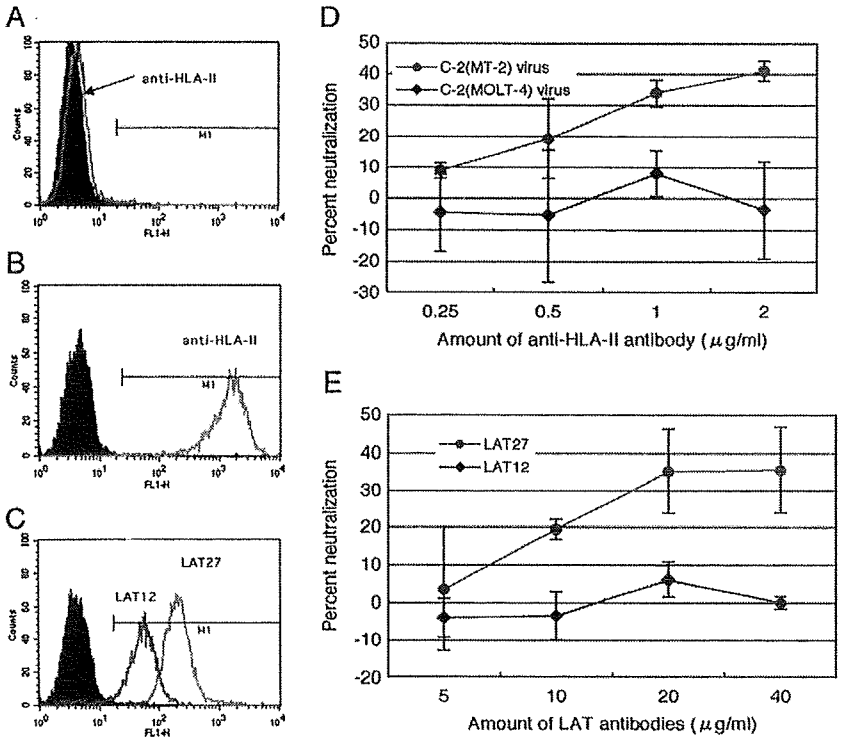

Fig. 4. Flow cytometric analysis of HLA-II expression in MOLT-4 (A) and MT-2 (B) cells, and HTLV-I gp46 expression in MT-2 cells (C). Neutralization of C-2(MT-2) (circles) and C-2(MOLT-4) (diamonds) viruses by anti-HLA-II (D) and neutralization of C-2(MT-2) viruses by LAT27 (circles) and LAT12 (diamonds) (E) are shown. The solid lines in panels D and E show the mean±SD of 6 independent experiments.

antibody at 2 g/ml neutralized 40% of the C-2(MT-2) viruses, whereas the C-2 viruses were not affected (Fig. 4D). C-2(MT-2) viruses were also neutralized by the neutralizing LAT27 antibody, but not by the non-neutralizing LAT12 antibody (Fig. 4E). However, 20–40 g/ml of the LAT27 antibody only neutralized 35% of the C-2(MT-2) viruses. In addition, the level of neutralization quickly reached a plateau with more than 20 g/ml of the antibody. Infection of C-2(MT-2) viruses in MAGI cells was almost completely blocked by 0.5 or T140, indicating that C-2(MT-2) viruses used HIV-1 gp120 and CXCR4 for the infection (data not shown). Nevertheless, HLA-II and HTLV-I gp46 on HIV-1 particles could be used as target molecules for neutralization of the virus by the respective antibodies.

One of the mechanisms proposed for HIV-1 neutralization by antibodies against non-HIV-1 molecules is the "coating theory," which suggests that a dense coat of antibodies over the virion surface could interfere with viral adsorption to cells by steric hindrance. However, treatment of C-2(MOLT-4) or C-2 (MT-2) viruses with the anti-HLA-II, LAT12 and LAT27 antibodies did not significantly inhibit the viral attachment to MOLT-4 cells (Fig. 5). As a positive control, 2 g/ml of the anti-V3 0.5 antibody suppressed C-2(MOLT-4) viral adsorption to the cells by only 50%, which could be partly explained by 0.5 mAb-mediated blocking of gp120 V3 binding to CXCR4. Other mechanisms, such as fluidity alterations in the viral envelope rather than steric hindrance, may be responsible for the HIV-1 neutralization by antibodies against non-HIV molecules.

Suppression of fluidization by neutralizing antibodies against non-HIV molecules

At 1 g/ml, the anti-HLA-II antibody strongly suppressed the envelope fluidity of C-2(MT-2) viruses (Figs. 2C and D; Fig. 6A), but did not suppress that of C-2 viruses (Fig. 6B). These findings were well correlated with the neutralization data (Fig. 4D). The anti-HLA-II suppressed the fluidity by 15% at 37 °C. Since the anti-HLA-II antibody (2 g/ml) was previously reported to suppress the membrane fluidity of MT-2 cells

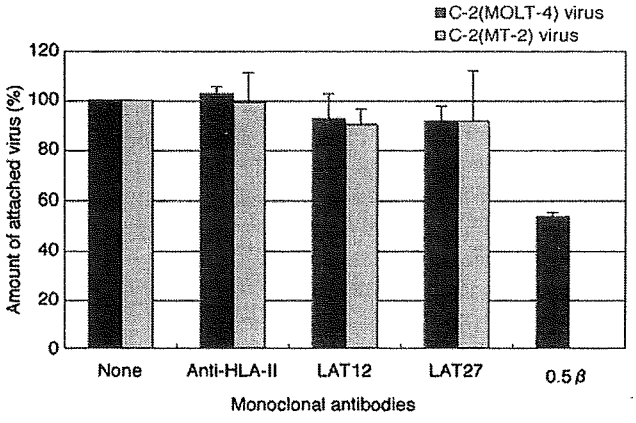

Fig. 5. Effects of MOPC21 (20 g/ml), anti-HLA-II (2 g/ml), LAT12 (20 g/ml), LAT27 (20 g/ml), and 0.5 (2 g/ml) on C-2(MOLT-4) or C-2(MT-2) virus adsorption on MOLT-4 cells. All experiments were carried out in triplicate, and the bars show the mean±SD.

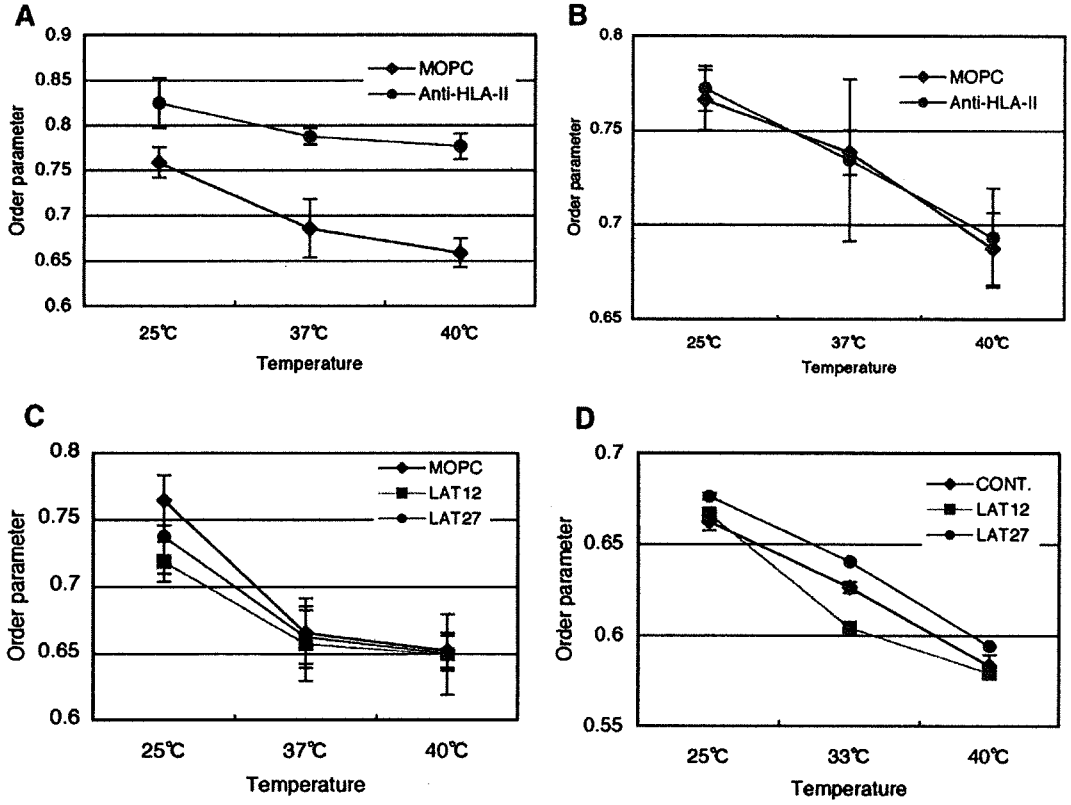

Fig. 6. Effects of 1 g/ml MOPC21 (diamonds) and 1 g/ml anti-HLA-II (circles) on envelope fluidity of C-2(MT-2) (A) and C-2 (B) viruses, and the effects of 10 g/ml LAT12 (squares) and 10 g/ml LAT27 (circles) on the fluidity of the viral envelope of C-2(MT-2) viruses (C) and plasma membrane of MT-2 cells (D). All measurements were carried out in triplicate and the solid lines show the mean±SD.

(Harada et al., 2004a), this antibody appears to universally lower the fluidity of lipid bilayers when it binds to membranes.

The LAT antibodies at 10 g/ml showed no significant suppression of fluidity in the C-2(MT-2) viruses (Fig. 6C). However, when MT-2 cells were treated with 10 g/ml of the LAT antibodies, the neutralizing LAT27 antibody suppressed the plasma membrane fluidity at all temperatures examined (Fig. 6D). In contrast, the non-neutralizing LAT12 antibody did not show any suppressive effects on MT-2 plasma membrane fluidity (Fig. 6D).

Discussion

The V3 loop of HIV-1 gp120 plays a critical role in determining the cell tropism of the virus (Clapham and McKnight, 2002). The loop is composed of approximately 35 amino acid residues with a global positive charge. An increase in the positive charge of the loop is thought to be associated with coreceptor usage (Hoffman and Doms, 1999; Moulard et al., 2000; Platt et al., 2001). A single amino acid change in V3 is able to switch viral coreceptor usage (CXCR4 or CCR5) (Hu et al., 2000; Shimizu et al., 1999). Furthermore, the V3 domain is considered to be the primary determinant of coreceptor usage (Cormier and Dragic, 2002) together with V1/V2 contributions (Dragic, 2001; Foda et al., 2001; Maeda et al., 2000). Anti-V3 antibodies strongly neutralize T-cell line-adapted strains of HIV-1 (Gorny et al., 2002; Zhang et al., 2002), and block the fusion induced by HIV-1 infection (Masuda et al., 1990) or gp120-expressing cells. The antibodies may neutralize viruses by interfering with several steps in the early phase of infection. It has been reported that anti-V3 mAbs interfere with the ability of gp120 and CD4 complexes to bind to CCR5 (Cormier et al., 2001). Thus, they act as receptor-blockers. However, HIV-1 neutralization by one or a few molecules of V3-targeted mAbs (Harada, 2002) and PAN (Armstrong et al., 1996) have been reported, suggesting the possibility of neutralizing effects after viral adsorption.

Engagement of the gp120 trimer with coreceptors induces gp41 rearrangement and exposure of the hydrophobic amino acid fusion domain, leading to fusion. The triggered fusion-activated gp41 structures are rod-like with a bundle of six -helices (Clapham and McKnight, 2002). It is conceivable that HIV-1 penetration into a cell requires a fusion-pore that is wide enough for the viral core to pass through. Accumulation of substantial numbers of fusion-activated gp41 structures with the help of fluidity of the lipid bilayer membrane must be necessary for this purpose. The formation of ring-like assemblies of fusion proteins has been reported in studies of rabies virus (Roche and Gaudin, 2002), baculovirus (Plonsky and Zimmerberg, 1996), influenza virus (Markovic et al., 2001) and Semliki Forest virus (Gibbons et al., 2003). Cell–cell fusion is temperature-dependent (Frey et al., 1995), and a time lag of 10–20 min between the six-helix bundle formation and fusion has been reported after transfer from 31.5 °C to 37 °C (Golding et al.,

2002). This indicates that the formation of a fusion pore requires a critical number of six-helix bundles.

The anti-HIV peptide T140 strongly inhibits X4 HIV-1 infection (Tamamura et al., 1998) through its specific binding to CXCR4, as shown by the finding that 1 M T140 could occupy most of the CXCR4 molecules on the cell surface. As a result, the binding of T140 to CXCR4 could prevent a loosely attached virus from forming additional multiple-site binding. In fact, the enhancement observed as PAE due to temperature shifts (25 °C to 37 °C and 25 °C to 40 °C) in the present study was strongly inhibited by T140, indicating that multiple-site binding was functioning and blocked by T140 occupation of CXCR4 molecules. We previously reported that PAE at 40 °C requires a time lag of 20–30 min before becoming apparent for blocking the enhancement by T140 after transfer from 25 °C to 40 °C (Harada et al., 2004a). This finding suggests that PAE requires the accumulation of gp120/receptor complexes through membrane fluidity, similar to the case for cell–cell fusion (Golding et al., 2002).

In the present study, V3-targeted 0.5 and 694/98-D mAbs inhibited the PAE of HIV-1 infection at 40 °C by 30–40% when the cells were pre-incubated with viruses at 25 °C. The PAN by anti-V3 antibodies was also observed when the shift was to 37 °C, but the infection was inhibited only by 10–20%. Thus, the antibodies mediate less potent PAN at 37 °C than at 40 °C, probably because the antibodies mainly suppress increased infectivity (PAE) due to increased temperature. Direct occlusion by the anti-V3 antibodies of open sites involved in the process of multiple-site binding to cells could be a way to prevent PAE at 40 °C. It is unknown whether these antibodies induce the detachment of adsorbed virions from cells. However, we found that PAE was only inhibited by 30–40% and a 10-fold higher dose (10 g/ml) of 0.5 showed no further inhibitory effect on the PAE, indicating that occupancy is not likely to happen in this case. Alternatively, the binding of the antibody to the viral surface could affect steric alterations to the viral envelope and restrain the envelope from enhancing the fluidity at 40 °C. In fact, we observed that binding of 0.5 and 694/98-D to C-2 viruses induced a more ordered or rigid envelope at 37 °C.

Neutralization of simian immunodeficiency virus (SIV) by anti-HLA and anti-hemagglutinin antibodies has previously been reported (Vzorov and Compans, 2000). In the present study, we also found that phenotype-mixed C-2(MT-2) viruses were neutralized by anti-HLA-II and LAT27 antibodies, although LAT27 exhibited a very weak neutralization activity. The reason why LAT27 is a neutralizing antibody, but LAT12 is not, remains unknown, although the binding affinity of LAT27 to MT-2 cells appeared to be stronger than that of LAT12. Two possible mechanisms are proposed for the neutralization of C-2 (MT-2) viruses by antibodies against non-HIV molecules. The first is the coating theory, which suggests that a dense coat of antibodies over the virion surface will interfere with viral adsorption to the cells, whereas the second is the steric alteration theory, which suggests that structural changes caused by binding of the antibodies will prevent penetration or uncoating of the virus. If the first mechanism is the case, adsorption of C-2 (MT-2) viruses, but not C-2(MOLT-4) viruses, should be blocked by antibodies against non-HIV molecules. However, we found that treatment of C-2(MOLT-4) and C-2(MT-2) viruses with anti-HLA-II, LAT12 and LAT27 antibodies did not significantly inhibit the viral adsorption. Instead, the anti-HLA-II antibody suppressed the envelope fluidity of C-2(MT-2) viruses, but not that of C-2 viruses. However, the neutralizing LAT27 antibody showed no suppressive effect on the fluidity of the C-2(MT-2) envelope, but did suppress the MT-2 plasma membrane fluidity, probably due to the increased HTLV-I gp46 expression on the MT-2 plasma membrane. Currently, the reason why the LAT27 neutralized C-2(MT-2) viruses is unknown. More sensitive techniques to measure minute changes of envelope fluidity might be required to explore the mechanism.

In the present study, the levels of neutralization (more than 90%) by 1 g/ml 0.5 and 694/98-D in conventional assays were much stronger than that of PAN (30–40% inhibition of PAE). PAN could be mainly exerted by suppression of the viral envelope fluidity. Apparently, anti-V3 antibodies have multifarious neutralization mechanisms, such as occupancy of V3 and stabilization of envelope fluidity. We found that the anti-HLA-II antibody showed 35% neutralization against C-2(MT-2) viruses at the concentration of 1 g/ml. This modest neutralization was only achieved by suppressing the fluidity. However, the significance or biological meaning of HIV-1 neutralization by anti-HLA-II antibodies or autoantibodies is the extraordinary protection revealed in studies on SIV-infected macaques vaccinated with cells expressing the same HLA molecules as those employed to culture the SIV used for the challenge (Arthur et al., 1995; Chan et al., 1992). Furthermore, antibodies against HLA are frequently present in HIV-exposed but uninfected individuals (Brown et al., 1997).

Suppressing the fluidity of the viral envelope could be one of the essential, but additional, mechanisms for virus neutralization because fluidity is indispensable for infectivity due to the required formation of multiple-site binding and a fusion pore (Harada, 2005; Harada et al., 2005, 2007). Antibodies may need substantial amounts of epitope molecules with high binding affinities on the plasma membrane or viral envelope to decrease its fluidity. The mechanism for fluidity suppression by antibodies is still unknown, but it is unlikely to be actin-dependent as the fluidity of the viral envelope was affected. The attachment of an antibody molecule, especially if it bridges adjacent subunits, is assumed to cause local structural alterations or topological changes of the integral protein, which spreads to the whole envelope or membrane, thereby stabilizing the fluidization for unknown reasons. Similarly, retrocyclin 2 was reported to immobilize surface proteins by cross-linking membrane glycoproteins (Leikina et al., 2005). Therefore, retrocyclin 2 exhibits inhibitory effects on viral fusion and entry. If the binding of the antibody itself is essential for lowering the fluidity, this cannot explain the presence of sensitizing (non-neutralizing) antibodies against viruses. Hence, a hypothesis has been proposed that viruses bear heterogeneous envelope molecules (Harada et al., 2004b), such as functional and nonfunctional gp120, and non-neutralizing antibodies only react with the nonfunctional gp120 (Poignard et al., 2003).

Furthermore, there must be specific molecules or epitopes that switch fluidization on or off after binding of the respective antibody. Further studies will be needed to clarify the mechanisms involved in modifying the fluidity of lipid bilayer membranes.

Materials and methods

Cells and culture

MOLT-4, MOLT-4/HIV-$1_{C\text{-}2}$, MOLT-4/HIV-$1_{esc.C\text{-}2}$ (Masuda et al., 1990) and MT-2 (Harada et al., 1985) cells were cultured in RPMI1640 medium (Gibco BRL, Grand Island, NY) supplemented with 10% heat-inactivated fetal bovine serum (FBS), 2 mM L-glutamine, 100 IU/ml of penicillin and 0.1 mg/ml streptomycin (complete medium). Multinuclear activation of a galactosidase indicator (MAGI) cells derived from HeLa-CD4/ long terminal repeat- -galactosidase cells (Kimpton and Emerman, 1992) were maintained in complete medium supplemented with 0.1 mg/ml G418 and 0.05 mg/ml hygromycin B. GHOST/CXCR4 cells derived from a human osteosarcoma cell line (HOS) were cultured in complete medium supplemented with 0.2 mg/ml G418, 0.05 mg/ml hygromycin B and 2 mg/ml puromycin as previously described (Cecilia et al., 1998).

Preparation of viruses

Plaque-cloned HIV-$1_{C\text{-}2}$ viruses (III_B X4 strain) and their 0.5 -escaped HIV-$1_{esc.C\text{-}2}$ viruses (Harada et al., 1985; Masuda et al., 1990) were obtained from 3-day-old culture supernatants of persistently infected MOLT-4/HIV-$1_{C\text{-}2}$ and MOLT-4/HIV-$1_{esc.C\text{-}2}$ cells, respectively. HTLV-I-transformed MT-2 cells were infected with C-2 viruses and cultured for 4 or 5 days. Progeny viruses in the supernatant were used as HIV-$1_{C\text{-}2(MT\text{-}2)}$. After filtration through a membrane (0.45 m pore size), the supernatants were stored at −80 °C until use. X4 envelope-pseudotyped viruses with a luciferase reporter gene (NL43-luc viruses) were produced by the calcium phosphate transfection method (Maeda et al., 2000). 293T cells were cotransfected with an envelope-deficient NL43 construct carrying the luciferase gene (pNL43-luc) and a pCXN2 vector expressing the envelope glycoprotein from pNL43.

Antibodies and reagents

A mouse IgG1 mAb, 0.5 , recognizing 24 amino acids in the V3 loop of gp120, was used (Matsushita et al., 1988). Three human anti-HIV mAbs were kindly provided by Dr. Susan Zolla-Pazner. Specifically, these mAbs were 694/98-D specific for the V3 region of gp120, 670-30D specific for the C5 region of gp120 and 246-D specific for the cluster I region of gp41 (Nyambi et al., 2000). An anti-HLA-II antibody (mouse anti-human HLA DR, DP, DQ) was purchased from Serotec (Oxford, UK) and stored at a concentration of 20 mg/ml in phosphate-buffered saline (PBS) at −80 °C. This antibody recognizes a monomorphic determinant common to each chain. Sodium azide showed no effects on the HIV-1 infectivity, adsorption, and membrane fluidity at 0.0002%, which was the maximum concentration used in this study. Mouse myeloma ascites IgG1 MOPC21 (Cappel, Cochranville, PA) was used as an IgG control. Rat LAT12 and LAT27 mAbs, which are non-neutralizing and neutralizing antibodies against HTLV-I, respectively, were also used (Tanaka et al., 1991). LAT27 recognizes amino acids 191–196 of HTLV-I gp46. A CXCR4 antagonist, T140, was kindly provided by Drs. H. Tamamura and N. Fujii (Tamamura et al., 1998). 5-Doxyl stearic acid (5-DSA) was purchased from Sigma-Aldrich (St. Louis, MO) and stored at a concentration of 20 mg/ml in ethanol at 4 °C until use.

Measurement of membrane fluidity in intact cells and viruses by electron spin resonance (ESR) spectroscopy

For ESR analyses, 1 ml of cells (7 10^6) or 50 ml of culture supernatant containing viruses (2–3 g of p24) were mixed with 1 ml of 60 g/ml 5-DSA or 25 ml of 90 g/ml 5-DSA in PBS, respectively, to make a final concentration of 30 g/ml, and incubated at 37 °C for 20 min (Sauerheber et al., 1980). The cells were washed thrice with PBS to remove the free spin label. The viruses were centrifuged at 114,000 *g* for 1 h at 4 °C in a 60 Ti Beckman rotor. The cell or virus pellets were resuspended in 40 l of PBS and drawn into capillary tubes. The ends of the tubes were sealed, before they were placed in quartz glass tubes and taken from the P3 facility. Spectra were recorded with a JES-RE1X ESR spectrometer (JEOL, Tokyo, Japan) equipped with a variable temperature control accessory. The instrument conditions were 2 min scan time, 5.0 mT sweep width, 0.1 mT field modulation width, 10 mW microwave power and 0.3 s time constant (Harada, 2005; Harada et al., 2005, 2007). Fig. 2 shows representative spectra, for which the outer hyperfine splitting indicates $2A_{//}$, and the inner one denotes 2A . The horizontal axis reflects the varying magnetic fields and the vertical axis represents the absorption of microwaves. The order parameter (*S*) was calculated as follows; $S=(A_{//}-A\ )/[A_{zz}-(A_{xx}+A_{yy})/2]=(A_{//}-A\ )/27.3G$.

Conventional neutralization and MAGI assay

Aliquots (200 l) of 2-fold-diluted antibodies (anti-HLA-II or LAT antibodies) were mixed with 200 l of C-2(MT-2) viruses, and incubated at 37 °C for 30 min. Next, aliquots (100 l/well) of the mixtures were seeded in triplicate on MAGI cells (8 10^4/well) that had been split into a flat-bottom 12-well plate on the previous day. The plate was incubated at 37 °C for 1 h with occasional shaking. After one wash with complete medium, 1 ml/well of complete medium was added, and the cells were cultured at 37 °C for 2 days before HIV-1-positive cells were stained by the MAGI assay. The infected cells were fixed with 1% formaldehyde and 2% glutaraldehyde in PBS for 5 min, washed twice with PBS, and incubated with staining solution (3 mM potassium ferrocyanide, 3 mM potassium ferricyanide, 1 mM $MgCl_2$ and 0.4 mg of X-Gal in PBS) at 37 °C for 40 min (Kimpton and Emerman, 1992). Doses of C-2

(MT-2) and C-2(MOLT-4) viruses were adjusted to make 100 to 200 positive cells per well without antibodies. The percent neutralization was calculated as follows: (1 − positive cells in test wells/positive cells in control wells) 100.

Blocking of post-attachment enhancement (PAE) and infectivity assay with luciferase readout

GHOST/CXCR4 cells (2.5 10^4 cells/well) that had been seeded into a flat-bottom 48-well plate on the previous day were infected with 100 l/well of NL43-luc pseudoviruses (50 ng p24/ml). Viral adsorption was allowed to take place at 25 °C for 1 h. After one wash with complete medium, the cells were incubated in the presence or absence of T140 or mAbs against HIV-1 at 37 °C or 40 °C for 1 h and then washed once (Harada et al., 2004a, 2005). Subsequently, the plate was incubated at 37 °C for 2 days, and the infected cells were lysed with 100 l/well of luciferase assay buffer (Promega, Madison, WI). The luciferase activity was measured by adding 50 l of luciferase assay substrate (Promega) to 10 l of cell lysate and reading the light activity in a luminometer (Lumat LB 9501/16; EG&G Berthold, Bad Wildbad, Germany) (Song et al., 2001).

Viral adsorption experiment

C-2(MOLT-4) or C-2(MT-2) viruses (400 l each, 10 ng p24/ml) were mixed with MOPC21, anti-HLA-II, LAT12, LAT27 and 0.5 antibodies at final concentrations of 20, 2, 20, 20 and 2 g/ml, respectively, and incubated at 37 °C for 30 min. MOLT-4 cells (10^6 cells/tube) were treated with 100 l/tube of each mixture in triplicate, and incubated at 37 °C for 1 h. Next, the cells were subjected to two extensive washes with PBS and lysed with 50 l/tube of lysis buffer. The amount of p24 was assessed by ELISA (Cellular Products, Buffalo, NY).

Flow cytometric analysis

MOLT-4 or MT-2 cells (10^6 cells/tube) were treated with 50 l of anti-HLA-II (10 g/ml), LAT12 (10 g/ml) and LAT27 (10 g/ml) antibodies at 4 °C for 1 h. After two washes with PBS, the cells were incubated with 50 l of fluorescein isothiocyanate (FITC)-conjugated goat antiserum against mouse or rabbit antibodies (Organon Teknika, West Chester, PA) for 1 h at 4 °C. After two washes with PBS, the cells were resuspended with PBS for analysis using a FACScan system (Becton Dickinson, Mountain View, CA) (Song et al., 2001).

Acknowledgments

We thank Dr. Susan Zolla-Pazner for the gift of the human anti-HIV monoclonal antibodies. This work was supported by the Ministry of Health, Labour and Welfare (Health Sciences Research Grants), and also supported in part by the Cooperative Research Project on Clinical and Epidemiological Studies of Emerging and Re-emerging Infectious Diseases (Renkei Jigyo: No. 78, Kumamoto University) of the Ministry of Education, Culture, Sports, Science and Technology (Monbu-Kagakusho) of Japan.

References

Armstrong, S.J., Mclnerney, T.L., McLain, L., Wahren, B., Hinkula, J., Levi, M., Dimmock, N.J., 1996. Two neutralizing anti-V3 monoclonal antibodies act by affecting different functions of human immunodeficiency virus type 1. J. Gen. Virol. 77, 2931–2941.

Arthur, L.O., Bess Jr., J.W., Urban, R.G., Strominger, J.L., Morton, W.R., Mann, D.L., Henderson, L.E., Benveniste, R.C., 1995. Macaques immunized with HLA-DR are protected from challenge with simian immunodeficiency virus. J. Virol. 69, 3117–3124.

Brown, L., Westby, M., Souberbielle, B.E., Szawlowski, P.W.S., Kemp, G., Hay, P., Dalgleish, A.G., 1997. Optimisation of a peptide-based indirect ELISA for the detection of antibody in the serum of HIV-1 seropositive patients. J. Immunol. Methods 200, 79–88.

Cecilia, D., KewalRamani, V.N., O'Leary, J., Volsky, B., Nyambi, P., Burda, S., Xu, S., Littman, D.R., Zolla-Pazner, S., 1998. Neutralization profiles of primary human immunodeficiency virus type 1 isolates in the context of coreceptor usage. J. Virol. 72, 6988–6996.

Chan, W.L., Rodgers, A., Hancock, R.D., Taffs, F., Kitchin, P., Farrar, G., Liew, F.Y., 1992. Protection in simian immunodeficiency virus-vaccinated monkeys correlates with anti-HLA class I antibody response. J. Exp. Med. 176, 1203–1207.

Clapham, P.R., McKnight, A., 2002. Cell surface receptors, virus entry and tropism of primate lentiviruses. J. Gen. Virol. 83, 1809–1829.

Cormier, E.G., Dragic, T., 2002. The crown and stem of the V3 loop play distinct roles in human immunodeficiency virus type 1 envelope glycoprotein interactions with CCR5 coreceptor. J. Virol. 76, 8953–8957.

Cormier, E.G., Tran, D.H., Yukhayeva, L., Olson, W.C., Dragic, T., 2001. Mapping the determinants of the CCR5 amino-terminal sulfopeptide interaction with soluble human immunodeficiency virus type 1 gp120-CD4 complexes. J. Virol. 75, 5541–5549.

Dragic, T., 2001. An overview of the determinants of CCR5 and CXCR4 co-receptor function. J. Gen. Virol. 82, 1807–1814.

Edwards, M.J., Dimmock, N.J., 2001. Hemagglutinin 1-specific immunoglobulin G and Fab molecules mediate postattachment neutralization of influenza A virus by inhibition of an early fusion event. J. Virol. 75, 10208–10218.

Foda, M., Harada, S., Maeda, Y., 2001. Role of V3 independent domains on a dualtropic human immunodeficiency virus type 1 (HIV-1) envelope gp120 in CCR5 coreceptor utilization and viral infectivity. Microbiol. Immunol. 45, 521–530.

Frey, S., Marsh, M., Gunther, S., Pelchen-Matthews, A., Stephens, S., Stegmann, T., 1995. Temperature dependence of cell–cell fusion induced envelope glycoprotein of human immunodeficiency virus type 1. J. Virol. 69, 1462–1472.

Gibbons, D.L., Erk, I., Reilly, B., Navaza, J., Kielian, M., Rey, F.A., Lepault, J., 2003. Visualization of the target-membrane-inserted fusion protein of Semliki Forest virus by combined electron microscopy and crystallography. Cell 114, 573–583.

Golding, H., Zaitseva, M., de Rosny, E., King, L.R., Manischewitz, J., Sidorov, I., Gorny, M.K., Zolla-Pazner, S., Dimitrov, D.S., Weiss, C.D., 2002. Dissection of human immunodeficiency virus type 1 entry with neutralizing antibodies to gp41 fusion intermediates. J. Virol. 76, 6780–6790.

Gorny, M.K., Williams, C., Volsky, B., Revesz, K., Cohen, S., Polonis, V.R., Honnen, W.J., Kayman, S.C., Krachmarov, C., Pinter, A., Zolla-Pazner, S., 2002. Human monoclonal antibodies specific for conformation-sensitive epitopes of V3 neutralize human immunodeficiency virus type 1 primary isolates from various clades. J. Virol. 76, 9035–9045.

Harada, S., 2002. Human immunodeficiency virus type 1 neutralization by a single molecule of V3-targeted antibody. Microbiol. Immunol. 46, 857–862.

Harada, S., 2005. The broad anti-viral agent glycyrrhizin directly modulates the fluidity of plasma membrane and HIV-1 envelope. Biochem. J. 392, 191–199.

Harada, S., Koyanagi, Y., Yamamoto, N., 1985. Infection of HTLV-III/LAV in

HTLV-I-carrying cells MT-2 and MT-4 and application in a plaque assay. Science 229, 563–566.

Harada, S., Akaike, T., Yusa, K., Maeda, Y., 2004a. Adsorption and infectivity of human immunodeficiency virus type 1 are modified by the fluidity of the plasma membrane for multiple-site binding. Microbiol. Immunol. 48, 347–355.

Harada, S., Yusa, K., Maeda, Y., 2004b. Heterogeneity of envelope molecules shown by different sensitivities to anti-V3 neutralizing antibody and CXCR4 antagonist regulates the formation of multiple-site binding of HIV-1. Microbiol. Immunol. 48, 357–365.

Harada, S., Yusa, K., Monde, K., Akaike, T., Maeda, Y., 2005. Influence of membrane fluidity on human immunodeficiency virus type 1 entry. Biochem. Biophys. Res. Commun. 329, 480–486.

Harada, S., Yokomizo, K., Monde, K., Maeda, Y., Yusa, K., 2007. A broad antiviral neutral glycolipid, fattiviracin FV-8, is a membrane fluidity modulator. Cell. Microbiol. 9, 196–203.

Hoffman, T.L., Doms, R.W., 1999. HIV-1 envelope determinants for cell tropism and chemokine receptor use. Mol. Membr. Biol. 16, 57–65.

Hu, Q., Trent, J.O., Tomaras, G.D., Wang, Z., Murray, J.L., Conolly, S.M., Navenot, J.M., Barry, A.P., Greenberg, M.L., Peiper, S.C., 2000. Identification of env determinants in V3 that influence the molecular anatomy of CCR5 utilization. J. Mol. Biol. 302, 359–375.

Kimpton, J., Emerman, M., 1992. Detection of replication-competent and pseudotyped human immunodeficiency virus with a sensitive cell line on the basis of activation of an integrated -galactosidase gene. J. Virol. 66, 2232–2239.

Klasse, P.J., Sattentau, Q.J., 2002. Occupancy and mechanism in antibody-mediated neutralization of animal viruses. J. Gen. Virol. 83, 2091–2108.

Leikina, E., Delanoe-Ayari, H., Melikov, K., Cho, M., Chen, A., Waring, A.J., Wang, W., Xie, Y., Loo, J.A., Lehrer, R.I., Chernomordik, L.V., 2005. Carbohydrate-binding molecules inhibit viral fusion and entry by cross-linking membrane glycoproteins. Nat. Immunol. 6, 995–1001.

Maeda, Y., Foda, M., Matsushita, S., Harada, S., 2000. Involvement of both the V2 and V3 regions of the CCR5-tropic human immunodeficiency virus type 1 envelope in reduced sensitivity to macrophage inflammatory protein 1 . J. Virol. 74, 1787–1793.

Markovic, I., Leikina, E., Zhukovsky, M., Zimmerberg, J., Chernomordik, L.V., 2001. Synchronized activation and refolding of influenza hemagglutinin in multimeric fusion machines. J. Cell Biol. 155, 833–844.

Masuda, T., Matsushita, S., Kuroda, M.J., Kannagi, M., Takatsuki, K., Harada, S., 1990. Generation of neutralization-resistant HIV-1 in vitro due to amino acid interchanges of third hypervariable env region. J. Immunol. 145, 3240–3246.

Matsushita, S., Robert-Guroff, M., Rusche, J., Koito, A., Hattori, T., Hoshino, H., Javaherian, K., Takatsuki, K., Putney, S., 1988. Characterization of a human immunodeficiency virus neutralizing monoclonal antibody and mapping of the neutralizing epitope. J. Virol. 62, 2107–2114.

Moulard, M., Lortat-Jacob, H., Mondor, I., Roca, G., Wyatt, R., Sodroski, J., Zhao, L., Olson, W., Kwong, P.D., Sattentau, Q.J., 2000. Selective interactions of polyanions with basic surfaces on human immunodeficiency virus type 1 gp120. J. Virol. 74, 1948–1960.

Nyambi, P.N., Nadas, A., Mbah, H.A., Burda, S., Williams, C., Gorny, M.K., Zolla-Pazner, S., 2000. Immunoreactivity of intact virions of human immunodeficiency virus type 1 (HIV-1) reveals the existence of fewer HIV-1 immunotypes than genotypes. J. Virol. 74, 10670–10680.

Platt, E.J., Kuhmann, S.E., Rose, P.P., Kabat, D., 2001. Adaptive mutations in the V3 loop of gp120 enhance fusogenicity of human immunodeficiency virus type 1 and enable use of a CCR5 coreceptor that lacks the amino-terminal sulfated region. J. Virol. 75, 12266–12278.

Plonsky, I., Zimmerberg, J., 1996. The initial fusion pore induced by baculovirus GP64 is large and forms quickly. J. Cell Biol. 135, 1831–1839.

Poignard, P., Moulard, M., Golez, E., Vivona, V., Franti, M., Venturini, S., Wang, M., Parren, P.W.H.I., Burton, D.R., 2003. Heterogeneity of envelope molecules expressed on primary human immunodeficiency virus type 1 particles as probed by the binding of neutralizing and nonneutralizing antibodies. J. Virol. 77, 353–365.

Roche, S., Gaudin, Y., 2002. Characterization of the equilibrium between the native and fusion-inactive conformation of rabies virus glycoprotein indicates that the fusion complex is made of several trimers. Virology 297, 128–135.

Sauerheber, R.D., Zimmermann, T.S., Esgate, J.A., VanderLaan, W.P., Gordon, L.M., 1980. Effects of calcium, lanthanum, and temperature on the fluidity of spin-labeled human platelets. J. Membr. Biol. 52, 201–219.

Shimizu, N., Haraguchi, Y., Takeuchi, Y., Soda, Y., Kanbe, K., Hoshino, H., 1999. Changes in and discrepancies between cell tropisms and coreceptor uses of human immunodeficiency virus type 1 induced by single point mutations at the V3 tip of the env protein. Virology 259, 324–333.

Song, W., Yahara, S., Maeda, Y., Yusa, K., Tanaka, Y., Harada, S., 2001. Enhanced infection of an X4 strain of HIV-1 due to capping and colocalization of CD4 and CXCR4 induced by capsianoside G, a diterpene glycoside. Biochem. Biophys. Res. Commun. 283, 423–429.

Tamamura, H., Xu, Y., Hattori, T., Zhang, X., Arakaki, R., Kanbara, K., Omagari, A., Otaka, A., Ibuka, T., Yamamoto, N., Nakashima, H., Fujii, N., 1998. A low-molecular-weight inhibitor against the chemokine receptor CXCR4: a strong anti-HIV peptide T140. Biochem. Biophys. Res. Commun. 253, 877–882.

Tanaka, Y., Zeng, L., Shiraki, H., Shida, H., Tozawa, H., 1991. Identification of a neutralization epitope on the envelope gp46 antigen of human T cell leukemia virus type I and induction of neutralizing antibody by peptide immunization. J. Immunol. 147, 354–360.

Trubey, C.M., Chertova, E., Coren, L.V., Hilburn, J.M., Hixson, C.V., Nagashima, K., Lifson, J.D., Ott, D.E., 2003. Quantitation of HLA class II protein incorporated into human immunodeficiency type 1 virions purified by anti-CD45 immunoaffinity depletion of microvesicles. J. Virol. 77, 12699–12709.

Verrier, F., Nadas, A., Gorny, M.K., Zolla-Pazner, S., 2001. Additive effects characterize the interaction of antibodies involved in neutralization of the primary dualtropic human immunodeficiency virus typel isolate 89.6. J. Virol. 75, 9177–9186.

Vzorov, A.N., Compans, R.W., 2000. Effect of the cytoplasmic domain of the simian immunodeficiency virus envelope protein on incorporation of heterologous envelope proteins and sensitivity to neutralization. J. Virol. 74, 8219–8225.

Zhang, P.F., Bouma, P., Park, E.J., Margolick, J.B., Robinson, J.E., Zolla-Pazner, S., Flora, M.N., Quinnan Jr., G.V., 2002. A variable region 3 (V3) mutation determines a global neutralization phenotype and CD4-independent infectivity of a human immunodeficiency virus type 1 envelope associated with a broadly cross-reactive, primary virus-neutralizing antibody response. J. Virol. 76, 644–655.

Zwart, G., Langeduk, H., Van Der Hoek, L., DeJong, J., Wolfs, T.F.W., Ramautarsing, C., Bakker, M., DeRonde, A., Goudsmit, J., 1991. Immunodominance and antigenic variation of the principal neutralization domain of HIV-1. Virology 181, 481–489.

Zwick, M.B., Wang, M., Poignard, P., Stiegler, G., Katinger, H., Burton, D.R., Parren, P.W.H.I., 2001. Neutralization synergy of human immunodeficiency virus type 1 primary isolates by cocktails of broadly neutralizing antibodies. J. Virol. 75, 12198–12208.

Microbiol Immunol 2008; **52**: 78–88
doi:10.1111/j.1348-0421.2008.00012.x

Human immunodeficiency virus type-1 vulnerates nascent neuronal cells

Hiroko Kitayama, Yoshiharu Miura, Yoshinori Ando and Yoshio Koyanagi

Laboratory of Viral Pathogenesis, Institute for Virus Research, Kyoto University, Kyoto 606-8507, Japan

Correspondence
Yoshio Koyanagi, Laboratory of Viral Pathogenesis, Institute for Virus Research, Kyoto University, 53 Shogoin-kawara-cho, Sakyo-ku, Kyoto 606-8507, Japan.
Tel: +81-75-751-4811; fax: +81-75-751-4812; email: ykoyanag@virus.kyoto-u.ac.jp

Received: 28 August 2007; accepted: 22 November 2007

List of Abbreviations: AIDS, acquired immunodeficiency syndrome; ART, antiretrovirus therapy; CNS, central nervous system; DG, dentate gyrus; EGFP, enhanced green fluorescent protein; FITC, fluorescein-isothiocyanate; GCL, granule cell layer; GFAP, glial fibrillary acidic protein; HIV-1, human immunodeficiency virus-1; NFP, neurofilament protein; NMDA, *N*-methyl-D-aspartate; mAb, monoclonal antibody; MDM, monocyte-derived macrophages; MF, mossy fiber; MLV, murine leukemia virus; MOI, multiplicity of infection; NeuN, neuronal nuclei; O4, oligodendrocyte O4; OHC, organotypic hippocampal slice culture; PBMC, peripheral blood mononuclear cells; PCL, pyramidal cell layer; PFA, paraformaldehyde; RT, room temperature; tat, transcriptional transactivator; TUNEL, terminal deoxynucleotidyl transferase (TdT)-mediated biotinylated UTP nick end labeling; TNF-α, tumor-necrosis factor α.

Key words
dentate gyrus, HIV-1, neuron, organotypic hippocampal slice cultures.

ABSTRACT

Macrophages or microglial cells are the major target cells for HIV-1 infection in the brain. The infected cells release neurotoxic factors that may cause severe neuronal cell damage, especially in the basal ganglia and hippocampus. In this study, we used rat OHC to examine the region-specific neuronal cell damage caused by HIV-1-infected macrophages. When OHC was cocultured with HIV-1-infected MDM, we found that neuronal cells at the GCL of the DG were preferentially killed via apoptosis, and that projection of MF from GCL to PCL of the CA3 region was severely disturbed. We marked precursor cells around the DG region by using an EGFP-expressing retrovirus vector and found that these cells lost the ability to differentiate into neurons when exposed to HIV-1-infected MDM. In the DG, new neurons are normally incorporated into GCL or PCL, while in the presence of HIV-1-infected MDM, mature neurons failed to be incorporated into those layers. These data indicate that the neurotoxic factor(s) released from HIV-1-infected macrophages impede(s) neuronal cell repair in brain tissue. This suggests that DG is the region of the hippocampus most vulnerable to neuronal damage caused by HIV-1 infection, and that its selective vulnerability is most likely due to the highly active neurogenesis that takes place in this region.

HIV infection is well known to be a cause for development of dementia. Most HIV-associated dementia is subcortical dementia due to predominant involvement of the basal ganglia, cerebral cortex, and hippocampus (1–3). Introduction of ART has improved the immunological condition of patients and reduced the incidence of HIV severe dementia in AIDS patients (1, 4, 5). However, due to improved survival rates among ART-treated patients and healthy HIV-infected individuals, prevalence rates of HIV-1 associated neurological disease continue to rise (1). These patients display milder neurological disease than the severe neurological disease seen in non-treated patients

(1, 2). Histopathological examination of autopsy samples from HIV-1 infected brains reveals the presence of multinucleated giant cells and loss of synapses and neurons (6).

Although the mechanisms involved in loss of synapses and neurons in these patients are not completely understood, some data support the contention that HIV-1 infected macrophages or microglial cells release neurotoxic factors such as viral products, excitotoxins, and/or cytokines and chemokines that damage neurons through multiple pathways (1, 7). These factors may also work to activate astrocytes which then produce chemokines and cytokines that affect neuronal function (8, 9). Such neurotoxic factors are likely to affect a diverse range of neurons in the most vulnerable areas of the CNS, including the hippocampus, frontal cortex and white matter (1). In HIV-infected individuals, viral and host factors released from HIV-1-infected macrophages might affect hippocampal mediated learning and memory formation (1, 10). It has been reported that macrophage-induced inflammation affected hippocampal plasticity in a murine model of HIV-1 encephalitis (11). However, there has been no longitudinal study on the pathogenesis of HIV-1 encephalopathy and therefore no information has been collected by *in vitro* assay regarding the mechanism of causation of milder HIV-1 associated neurological disease.

As an *in vitro* model of HIV-1 encephalopathy that mimics its pathogenesis *in vivo*, OHC were employed in the present study. OHC would provide an alternative model to examine neuronal cell function in the hippocampus (12). As cellular composition, architecture and connections within the hippocampus are well preserved in OHC, the microenvironment in which the cells are immersed is similar to that in living animals (13–15). Although a few exceptions have been found, probably as a result of afferent deprivation of neuronal signals (16, 17), neurons in slice culture maintain their physiological arrangement and the capability to transmit signals (12). In addition, neurogenesis has been reported to occur in hippocampal slice cultures (18, 19). Therefore, slice cultures have been widely used to study morphology and plasticity of the hippocampus. Since HIV does not infect cells with a neuronal lineage, it was considered appropriate to use small animal-derived OHC in combination with HIV-1-infected human macrophages to study pathological changes in the brain of HIV-1-infected individuals.

In the present study, we established an *in vitro* model of HIV-1 encephalopathy using rat OHC exposed to HIV-1-infected MDM. This model reproduced pathological alterations such as neuronal apoptosis, loss of synapses and activation of astrocytes or microglial cells. More importantly, granule cells in the DG, where active neurogenesis occurs, were found to be predominantly damaged at an early stage, and neuronal cell differentiation was found to be disturbed by viral and/or host factors released from HIV-1-infected MDM. This culture system will be useful for understanding the pathology of HIV-1 encephalopathy in the hippocampus.

MATERIALS AND METHODS

OHC and cocultivation with HIV-1-infected macrophages

OHC were prepared from postnatal day seven Wister Hannover GALAS rats (CLEA, Osaka, Japan) as previously described (18). The experiments were carried out in accordance with the guidelines of Kyoto University for animal experimentation. After decapitation, the brain was removed and transversely sliced at the hippocampus into a 350 μm thickness on a McIlwain tissue chopper (Mickle Laboratory Engineering, Guildford, UK). The slices were cultured on porous translucent membrane (Millicell-CM, Millipore, Bedford, MA, USA) at 34°C and the culture medium was changed three times a week. The culture medium consisted of 50% OPTI-MEM (Invitrogen, Carlsbad, CA, USA), 25% heat inactivated horse serum (Invitrogen) and 25% Hank's balanced salt solution (Invitrogen) supplemented with D-glucose (5 g/L, Wako, Osaka, Japan), penicillin and streptomycin (100 units/ml, 100 μg/ml, respectively, Invitrogen). Two weeks after initiation of culture, slices were cocultured with HIV-1_{JRFL} (20)-infected (MOI 1.0) or uninfected MDM isolated from PBMC of HIV-1 seronegative healthy donors, across the porous membrane in culture medium for another two weeks. The concentration of p24 antigen was measured by ELISA (RETROtek, ZeptoMetrix, Buffalo, NY, USA).

Retrovirus vector transduction

An MLV-based vector, SRα-EGFP (21), was derived from SRαL*thy* (22) by replacing the murine thy 1.2 gene with EGFP. Vector was generated as described before (21). The titer of vector was 1.7×10^7 infectious units per milliliter. Slices were inoculated with SRα-EGFP by microinjection (FemtJet and Inject Man NI2, Eppendorf, Hamburg, Germany) in the suprapyramidal region of the GCL at the DG (18). Then, slices were cultured without, or with uninfected or HIV-1-infected MDM, as described above.

Staining dead cells in OHC

After removal of culture medium, slices were incubated at 34°C with culture medium containing SYTOX Green dye (Invitrogen) for 30 min and then samples were examined using a fluorescent microscope (Nikon TS100, Nikon, Tokyo, Japan) using a GFP filter with 5× objective.

Antibodies

MAb against NeuN, nestin and O4 were purchased from Chemicon (Temecula, CA, USA). MAb against NFP and rat CD68 (clone ED1) were purchased from DakoCytomation (Carpinteria, CA, USA), and Serotec (Oxford, UK), respectively. A rabbit polyclonal antibody against GFAP was purchased from DakoCytomation. A rat mAb against EGFP was purchased from Nakarai (Kyoto, Japan). A biotin-conjugated goat anti-mouse IgM was purchased from Chemicon. Alexa Fluor 488-, 594-conjugated goat anti-mouse/rabbit IgG and Alexa Fluor 594-conjugated streptavidin were obtained from Invitrogen. An FITC-conjugated goat anti-rat IgG was obtained from Jackson Immuno Research Laboratories (West Grove, PA, USA).

Immunohistochemistry

Slices were fixed by immersion in 4% PFA for one hour at 4°C, and then incubated with blocking buffer containing 5% normal goat serum Vector Laboratories (Burlingame, CA, USA) and 0.3% Triton X-100 at 4°C overnight, followed by incubation with primary antibodies against the following molecules; NeuN, EGFP, NFP, rat CD68, O4, or GFAP at 4°C overnight in blocking solution. Sample stained with antibody against O4 was further incubated with biotin-conjugated anti-mouse IgM antibody at 4°C overnight. These samples were subsequently incubated at RT for another six hours with fluorescent dye conjugated secondary antibodies; Alexa Fluor 594-conjugated anti-mouse/rabbit IgG with or without FITC-conjugated anti-rat IgG or Alexa Fluor 594-conjugated streptavidin. Nuclei were stained using Hoechst33342 (Invitrogen). Each sample was examined under a fluorescent microscope (Leica CTR6500, Leica Microsystems, Heidelberg, Germany) using a Texas Red filter with 5× and 10× objectives, and a confocal laser microscope (TCS SP2 AOBS, Leica Microsystems) using 405, 488 or 543 nm excitations with 10×, 20× and 40× objectives. The quantification of fluorescent intensity was done following the protocol supplied by the manufacturer (LCS Lite software, Leica Microsystems).

TUNEL staining

Slices were fixed by immersion in 4% PFA for one hour at 4°C, treated with 20 mg/ml proteinase K in 50 mM Tris-HCl buffer at 37°C for 15 min, and then fixed again with 4% PFA for 30 min at 4°C. Following permeabilization with 0.3% Triton X-100 for one hour at RT, the samples were incubated with TdT solution (TdT buffer, 25 mM $CoCl_2$, TdT [Terminal Transferase recombinant, Roche Applied Science, Indianapolis, IN, USA], biotin-16-2′-deoxy-uridine-5′-triphosphate [Roche Applied Science]) at 37°C for four hours. After washing, samples were stained with anti-NeuN antibody as described above and subsequently incubated with fluorescent dye conjugated secondary antibodies: Alexa Fluor 488-conjugated anti-mouse IgG (NeuN) and streptavidin Alexa Fluor 594-conjugated (TUNEL). Nuclei were stained using Hoechst33342 at RT for six hours. Samples were examined under a confocal laser microscope using 405, 488 and 543 nm excitations with 20× and 40× objectives as described above.

RESULTS

Microscope analysis of OHC exposed with HIV-MDM

Since OHC is known to preserve morphological features of the CNS for at least one month, we used it to explore tissue damage caused by HIV-1 protein or humoral host factor produced by HIV-1-infected macrophages in the hippocampus. Typical cellular arrangement of granule cells was reconstituted in slices on a porous membrane 14 days after initiation of culture and slices were then exposed to HIV-1_{JRFL}-infected or uninfected MDM across the porous membrane for another 14 days. The laminated structure and morphological organization of slices cocultured with or without uninfected MDM was maintained during the 14 days (data not shown), while the slice exposed to HIV-1-infected MDM (HIV-MDM) was found to gradually become thinner (Fig. 1A). Although cell morphology of MDM was not changed by HIV-1 infection, high concentrations of HIV-1 even greater than 200 ng p24 antigen per milliliter were found in culture supernatant (Fig. 1A and B). In addition, moderate thinning down of slices was induced by exposure to culture supernatant of lower concentrations of p24 antigen (below 20 ng per milliliter) from HIV-1-infected MDM (data not shown). These results suggest that HIV-1-infected MDM produce factor(s) that impair the maintenance of neuronal tissue architecture.

HIV-1-induced region-specific damage of neuronal cells in the hippocampus

To examine which region was affected by HIV-1-infected MDM, OHC was cultured in the presence of a non-permeable staining reagent, SYTOX, and cell damage was examined. Two days after exposure to HIV-1-infected MDM, severe cell damage in the neuronal cell layer was found (Fig. 2A), suggesting that neurons in these regions were predominantly harmed at an early stage after exposure to HIV-1-infected MDM. Fourteen days after exposure, we found severe loss of neurons especially at the GCL of the DG as revealed by staining with antibody

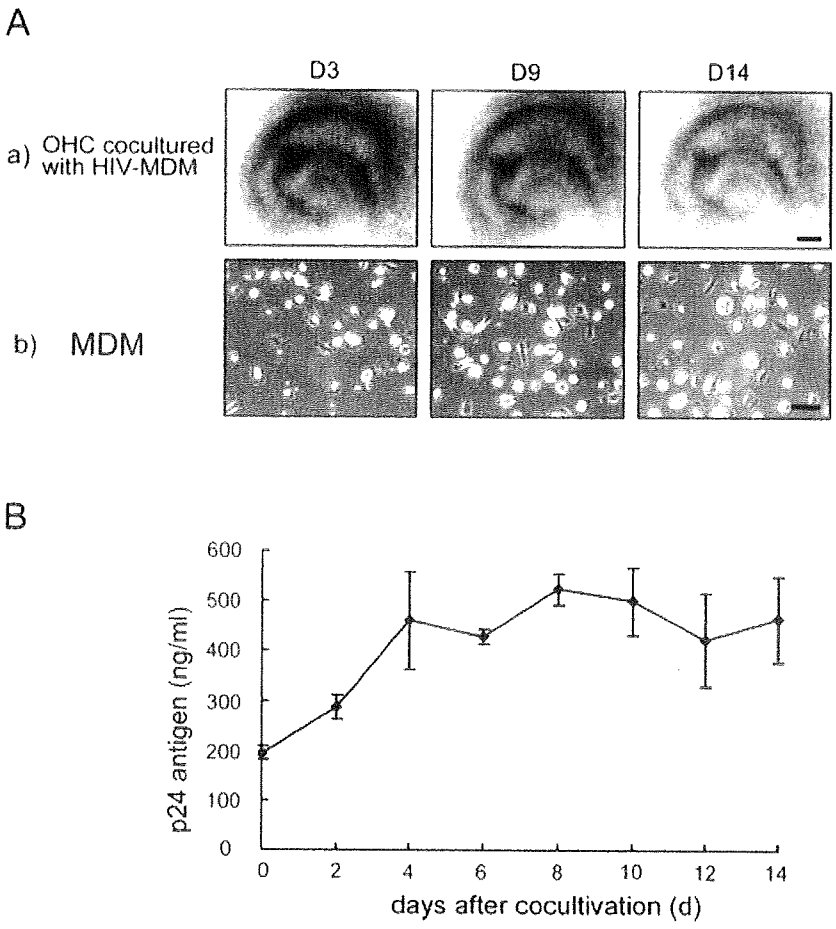

Fig. 1. Longitudinal alteration of OHC exposed to HIV-1-infected MDM. (A) OHC was cultured in the presence of HIV-1-infected MDM for two weeks. Microscopic examination was performed at days (D) 3, 9 and 14 after cocultivation. The slices gradually became thinner and cells were shed from them (a), though morphology of MDM was not affected by HIV-1 infection (b). Scale bar: 500 μm (a), 100 μm (b). (B) Large amount of HIV-1 was produced by HIV-1-infected MDM during cocultivation. X-axis is days after cocultivation and Y-axis is p24 concentration in supernatant of culture medium measured by ELISA.

against NeuN (Fig. 2B). Loss of GCL neurons was also found by staining with antibody against Calbindin D28K, one of the calcium binding proteins expressed specifically in GCL neurons (data not shown). Three-dimensional analysis revealed that the number of NeuN positive neurons clearly decreased and thickness of the sample became thinner in slices exposed to HIV-MDM compared to those without cocultivation (Fig. 2C). This change could not be found when OHC was exposed to HIV-1-infected HeLa-derived cells (data not shown), indicating that loss of neurons was specific to HIV-1-infected MDM and that exposure to HIV-1-infected MDM was more effective in reproducing the pathological alteration of HIV-1 encephalopathy. These results suggest that humoral factor(s) produced from HIV-1-infected MDM preferentially damage cells in the DG.

Neuronal apoptosis in the DG induced by HIV-1-infected MDM

To investigate the mechanism involved in the reduction in number of neurons especially at the DG region, we next carried out TUNEL staining to examine whether these cells were killed via apoptosis. There were many TUNEL positive cells in $NeuN^+$ neurons localized at the DG region in slices exposed to HIV-1-infected MDM (Fig. 2D and E). By contrast, in slices exposed to uninfected MDM, there were less TUNEL positive neurons in PCL and GCL. Furthermore, in slices exposed to uninfected MDM, there was no difference in the number of TUNEL positive cells between PCL (CA1 and CA3) and GCL (DG) (Fig. 2E). These data indicate that granule cells in the DG area are highly susceptible to apoptosis which is probably induced by neurotoxic humoral factor released from HIV-1-infected MDM.

Synaptic loss of GCL neurons induced by HIV-1-infected MDM

We assumed that other mechanisms besides neuronal apoptosis induced neuronal damage at the DG in OHC. To confirm this assumption, we used NFP as a marker to visualize neuronal filaments such as axons and dendrites. In slices exposed to HIV-1-infected MDM, expression of NFP was severely disturbed at the DG region (Fig. 2F and G).

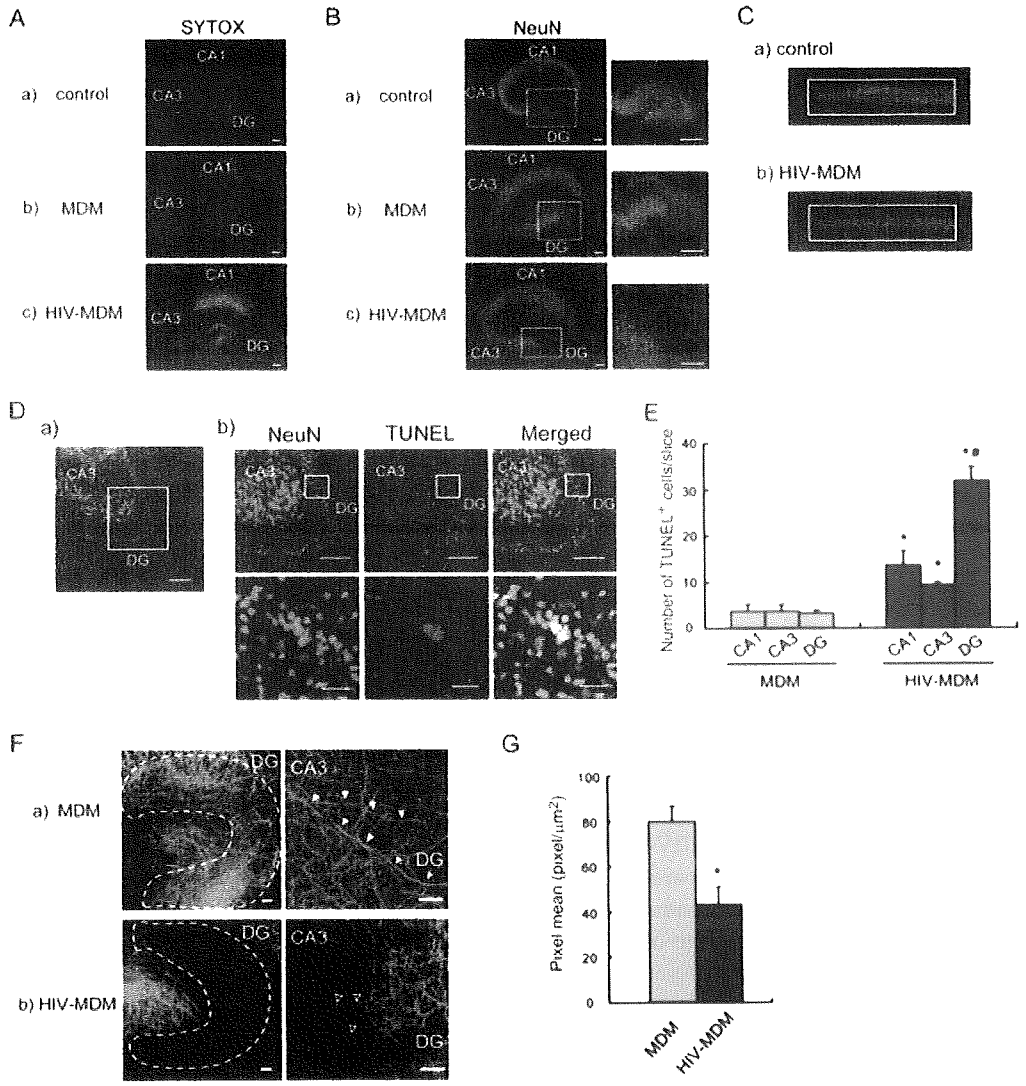

Fig. 2. Neurotoxic effect in OHC exposed to HIV-1-infected MDM. (A) Neurons in the CA1 and DG were harmed at early stage after the initiation of the exposure to HIV-1-infected MDM. Slices were cultured without (a; control) or with uninfected (b; MDM) or HIV-1-infected MDM (c; HIV-MDM) for two days and stained with SYTOX. CA1: CA1 region, CA3: CA3 region, DG: dentate gyrus. Scale bars: 100 μm. (B) Severe loss of neurons at the GCL of the DG was found in OHC exposed to HIV-1-infected MDM. Slices were cultured without (a; control) or with uninfected (b; MDM) or HIV-1-infected MDM (c; HIV-MDM) for 14 days and stained with antibody against NeuN. Rectangular regions were enlarged. CA1: CA1 region, CA3: CA3 region, DG: dentate gyrus. Scale bars: 100 μm. (C) Thinning of slices and loss of neurons were found by three-dimensional analysis in OHC exposed to HIV-1-infected MDM. Slices were cultured without (a; control) or with HIV-1-infected MDM (b; HIV-MDM) for 14 days and stained with NeuN (neuron) and Hoechst33342 (nuclei). The x-z plane of slices was imaged using a fluorescent microscope. (D) Neuronal apoptosis was induced by HIV-1-infected MDM. Slices cultured with HIV-1-infected MDM were stained with TUNEL (red) and anti-NeuN antibody (green), and nuclei were stained with Hoechst33342 (blue). A low magnification image is shown in left panel (a), and a high magnification image is shown in right panel (b). Rectangular regions were enlarged. CA3: CA3 region, DG: dentate gyrus. Scale bars: 150 μm (a), 100 μm (b, upper panels), 25 μm (b, lower panels). (E) Neuronal apoptosis was induced especially at the GCL of the DG. The numbers of TUNEL positive neurons were counted at three areas (CA1, CA3 and DG) of the slices cultured with uninfected (MDM) or HIV-1-infected MDM (HIV-MDM). Y-axis indicates the number of TUNEL positive neurons in slice.*: $P < 0.01$ versus each area of MDM, #: $P < 0.01$ versus CA1 and CA3 in HIV-MDM. (F) Loss of synapses was induced in GCL neurons by HIV-1-infected MDM. Slices cultured with uninfected (a; MDM) or HIV-1-infected MDM (b; HIV-MDM) were stained using antibody against NFP and neuronal filaments were visualized. Low magnification images are shown in left panels, and high magnification images in right panels. The area enclosed by the dotted line indicates the DG area. Long axons were formed (filled arrowheads) in GCL neurons at DG and they projected to CA3 in slice cultured with uninfected MDM (a). Conversely, axons were severely damaged (open arrowheads) in GCL neurons of DG in slice cultured with HIV-1-infected MDM (b). Scale bars: 50 μm. (G) Pixel mean of the signal of NFP-stained samples was significantly decreased in the slices cultured with HIV-1-infected MDM (HIV-MDM). *: $P < 0.01$ versus uninfected MDM (MDM).

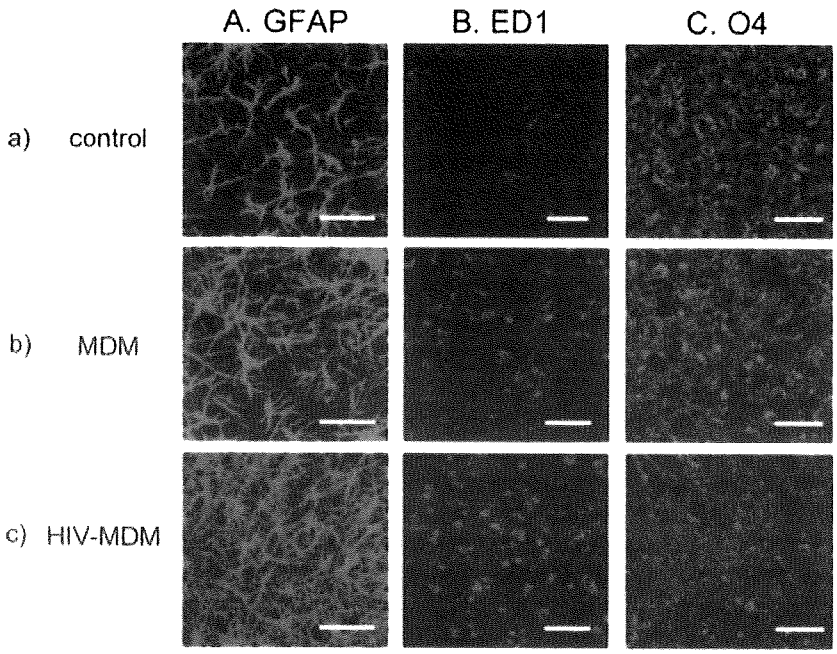

Fig. 3. Abnormality in astrocytes, microglial cells, and oligodendrocytes. Slices were cultured without (a; control) or with uninfected (b; MDM) or HIV-1-infected MDM (c; HIV-MDM) for 14 days and stained using antibodies against GFAP (A), ED1 (B) and oligodendrocyte O4 (C). The number of astrocytes increased in the presence of HIV-1-infected MDM (A), and the number of microglial cells increased and morphological changes were found when exposed to HIV-1-infected MDM (B). Conversely, oligodendrocytes were damaged by HIV-1-infected MDM (C). Scale bars: 50 μm.

Furthermore, the MF, collateral sprouting of dentate granule cell axons which form powerful excitatory synapses onto the proximal dendrites of CA3 pyramidal cells (23), were severely damaged in slices exposed to HIV-1-infected MDM (Fig. 2F, open arrowheads) as compared to uninfected MDM (Fig. 2F, filled arrowheads), indicating that HIV-1-infected MDM induce malformation of neuronal filaments and abnormality of synaptic projection onto neurons.

Activation of astrocytes or microglial cells and depletion of oligodendrocytes by HIV-1-infected MDM

We reproduced neuronal tissue damage through neuronal apoptosis and axonal malformations by exposure to HIV-1-infected MDM in the region of the DG. Other types of cells in OHC, which also includes astrocytes, microglial cells and oligodendrocytes, were also examined. It has been reported that astrocytes and microglial cells are extraordinarily activated in the brains of HIV-1 encephalopathy patients (2). From examination of GFAP (astrocyte marker), rat CD68 (microglial cell marker) and O4 (oligodendrocyte marker) expressions using immunofluorescence techniques, we found enlarged astrocytes and microglial cells in the slices exposed to HIV-1-infected MDM, indicating that astrocytes and microglial cells were activated (Fig. 3A and B). In addition, in the slices exposed to uninfected MDM, astrocytes and microglial cells were slightly enlarged, suggesting that both uninfected and HIV-1-infected MDM produce the factor(s) that induce activation of astrocytes and microglial cells (Fig. 3A and B). By contrast, the number of oligodendrocytes was clearly decreased in slices exposed to HIV-1-infected MDM, indicating that oligodendrocytes were preferentially damaged as seen in neurons by HIV-1-infected MDM (Fig. 3C). These results indicate that OHC cocultured with HIV-1-infected MDM is an adequate model for investigation of the molecular mechanism of HIV-1 encephalopathy.

Disablement of neuronal cell differentiation by HIV-1-infected MDM

It has become known that active neurogenesis occurs in the DG region of the hippocampus throughout the lifespan and that it is crucial for formation of neuronal plasticity (24). Many neuronal and glial progenitor cells or stem cells reside in the region and intrinsic and spontaneous neurogenesis are reported to take place at the DG in OHC (18, 19). In a healthy hippocampus, damaged neurons are continuously replaced by new cells generated at the DG region. However, in HIV-1-infected MDM-exposed slices, the damaged cells as shown in Figure 2 might accumulate as a result of weakened replacement. There could be two explanations for this observation. One is that the total number of precursors including progenitor cells and stem cells in DG decrease as a result of exposure to HIV-1-infected MDM. Another is that HIV-1-infected MDM interferes with the ability of precursor cells to differentiate and migrate.

To examine the first possibility, progenitor cells in the slices were stained with antibody against nestin, which is expressed predominantly in precursors including stem or progenitor cells of the CNS. We found similar numbers of nestin$^+$ precursor cells in slices exposed to either uninfected or HIV-1-infected MDM (Fig. 4A-a, b), indicating that factor(s) produced from HIV-1-infected MDM did not preferentially kill the precursors. To examine the second possibility, we labeled endogenous precursors in the slices using EGFP-expressing MLV vector (SRα-EGFP), which was microinjected into the suprapyramidal region of the GCL. Since MLV only infects dividing cells, and its DNA is incorporated into the host DNA, newly divided cells would specifically express EGFP. After inoculation with SRα-EGFP, slices were exposed to HIV-1-infected or uninfected MDM or not exposed to MDM at all. The total numbers of EGFP-expressing cells in all slices were similar irrespective of exposure of HIV-1-MDM or not for 2 weeks post inoculation (data not shown). To examine the ability of neuronal cell to differentiate, slices were fixed and stained with anti-NeuN antibody (neuron marker) and anti-EGFP antibody. In the slices cultured with uninfected MDM, some EGFP$^+$ cells also expressed NeuN and were incorporated into the GCL or PCL (Fig. 4B-a), and those cells had axon-like processes (Fig. 4B-a, filled arrowheads). Measurement of the numbers of EGFP$^+$ NeuN$^+$ neurons incorporated into the GCL or PCL revealed that half of EGFP$^+$ cells were neurons and those cells were incorporated into neuronal cell circuit in slices cultured with or without uninfected MDM (Fig. 4C). By contrast, in slice exposed to HIV-1-infected MDM, the majority of EGFP$^+$ cells were not incorporated into the GCL or PCL (Fig. 4B-b and C). Furthermore, EGFP$^+$ cells which were not incorporated into those layers did not express NeuN (Fig. 4B-c and C), indicating that EGFP$^+$ cells could not differentiate into mature neurons and that they might have differentiated into other cell types. These results indicate that maintenance of neuronal cell circuits is disturbed by exposure to HIV-1-infected MDM through inhibition of neuronal cell differentiation, but not by elimination of their progenitors in the DG.

DISCUSSION

In this study, we established a cocultivation system employing HIV-1-infected MDM and rat OHC that reproduces pathologic changes of HIV-1 encephalopathy. Neuronal dysfunctions including neuronal apoptosis and synaptic loss were produced especially in the GCL of the DG region in the hippocampus. Furthermore, in the DG, the differentiation of precursor cells into neurons was inhibited by exposure to HIV-1-infected MDM. These results highlight that the DG is profoundly susceptible to HIV-1 caused neuronal damage, and that HIV causes hippocampal dysfunction through damaging preexisting mature neurons and inhibiting the production of new neurons.

It has been reported that culture systems of a combination of OHC and HIV-1-encoded proteins, such as HIV-1-envelope glycoprotein 120 (gp120) or Tat, are useful for the study of HIV-1-induced neuronal damage (25–27), and that neuronal toxicity is induced by those viral proteins. Those culture systems are satisfactory for understanding the mechanisms by which a single protein affects maintenance of neuronal tissue. However, in the brain of HIV-1-infected patients, there are several viral proteins as well as host factors released from HIV-1-infected macrophages or microglial cells. Our coculture system using OHC and HIV-1-infected macrophages may reflect the brain damage which is concomitantly induced by several viral proteins and/or many host factors released from HIV-1-infected MDM. The combination of OHC and HIV-1-infected MDM may be more effective for identifying the mechanisms of HIV-1 encephalopathy. Moreover, in our coculture system, OHC might be exposed to high concentrations of viral and host factors and neuronal damage or degeneration thus induced, though neuronal damage was also found from exposure to a lower concentration of p24 antigen of culture supernatant. In the HIV-1-infected brain, HIV-1-infected macrophages penetrate across the blood-brain-barrier (2). More severe damage is induced around the area invaded by infected macrophages compared to uninvaded areas, as shown in simian immunodeficiency virus-infected brain samples (28). Our coculture system might reflect alterations which are closely related to those in areas invaded by HIV-1-infected macrophages.

Infected macrophages and microglial cells are known to be major HIV producers. They are also known to release viral proteins that can be deleterious to the CNS. HIV-1gp120, Tat and viral protein R have been shown to be toxic to neurons (29–33). HIV-1 gp120 interacts with cellular receptors and alters the signaling of the glutamate pathway. The signal induces cytokine production that can damage large number of neurons and affect the activation state of microglial cells and astrocytes (1). Nanomolar concentrations of gp120 have been reported to interact with the glycine binding site of the NMDA receptor (34). One possible molecular mechanism for gp120-induced neurotoxicity is that gp120 might induce glutamate-mediated excitotoxicity and initiate caspase cascades (35). Another viral protein Tat directly enters granule cells in the hippocampus and causes neurotoxicity (30). The neurotoxic effects of Tat seem to be mediated by interactions with a polyamine-sensitive site of the NMDA receptor in OHC (27). Infected cells also produce other neurotoxic